Pan-cancer survey of tumour mass dormancy and underlying mutational processes

Anna Julia Wiecek[1,†], Daniel Hadar Jacobson[1,†], Wojciech Lason[1,†], Maria Secrier[1*]

[1]UCL Genetics Institute, Department of Genetics, Evolution and Environment, University College London, UK

[†]These authors have contributed equally to this work and share first authorship

*** Correspondence:**
Maria Secrier
m.secrier@ucl.ac.uk

Keywords: tumour mass dormancy, immunity, angiogenesis, mutational signatures, APOBEC, hypoxia

ABSTRACT

Tumour mass dormancy is the key intermediate step between immune surveillance and cancer progression, yet due to its transitory nature it has been difficult to capture and characterise. Little is understood of its prevalence across cancer types and of the mutational background that may favour such a state. While this balance is finely tuned internally by the equilibrium between cell proliferation and cell death, the main external factors contributing to tumour mass dormancy are immunological and angiogenic. To understand the genomic and cellular context in which tumour mass dormancy may develop, we comprehensively profiled signals of immune and angiogenic dormancy in 9,631 cancers from the Cancer Genome Atlas and linked them to tumour mutagenesis. We find that immunological and angiogenic dormancy are pervasive, non-exclusive programmes in cancer that can be captured in 16.5% of bulk sequenced tumours, with a frequency of up to 33% in certain tissues. Mutations in the *CASP8* and *HRAS* oncogenes were positively selected in dormant tumours, suggesting an evolutionary pressure for controlling cell growth/apoptosis signals. By surveying the mutational damage patterns left in the genome by known cancer risk factors, we found that ageing-induced mutations were relatively depleted in these tumours, while patterns of smoking and defective base excision repair were linked with increased tumour mass dormancy. Furthermore, we identified a strong link between APOBEC mutagenesis and dormancy, which comes in conjunction with immune exhaustion and may partly depend on the expression of the angiogenesis regulator *PLG* as well as interferon and chemokine signals. Tumour mass dormancy also appeared to be impaired in hypoxic conditions in the majority of cancers. The microenvironment of dormant cancers was enriched in cytotoxic and regulatory T cells, as expected, but also in macrophages and showed a reduction in inflammatory Th17 signals. Finally, tumour mass dormancy was linked with improved patient survival outcomes. Our analysis sheds light into the complex interplay between dormancy, exhaustion, APOBEC activity and hypoxia, and sets directions for future mechanistic explorations.

1 Introduction

Tumour evolution is shaped by a variety of internal and external forces that act at different stages during cancer development, sometimes in an antagonistic manner, and drive distinct trajectories to advanced disease (McGranahan and Swanton 2017; Gerlinger et al. 2014; Temko et al. 2018). Within this rapidly changing context, adaptation of cancer cells is paramount for survival and much of it is achieved through cellular plasticity (Yuan, Norgard, and Stanger 2019). As a manifestation of this plasticity, cancer dormancy has emerged as an important contributor to the early stages of tumour development, as well as to cancer progression and metastatic dissemination (Phan and Croucher 2020; Jahanban-Esfahlan et al. 2019; Park and Nam 2020). Its two facets, cellular dormancy driven by arrest in the G0 state of the cell cycle (Phan and Croucher 2020), and tumour mass dormancy (TMD), described as an equilibrium between cell proliferation and cell death shaped by the microenvironment that constrains tumour growth (Aguirre-Ghiso 2007; H.F. Wang et al. 2019; Holmgren, O'Reilly, and Folkman 1995), are complementary but distinct mechanisms that contribute to the plasticity of cancer expansion (Huang 2021; Shen and Clairambault 2020). The former concept of was coined already in 1954 by Geoffrey Hadfield (HADFIELD 1954) and has since led to the generation of more detailed mechanistic insights explaining its regulation by the DREAM complex (Sadasivam and DeCaprio 2013; MacDonald et al. 2017; Kim et al. 2021), with key dependencies on the p53/p21 activation axis (Itahana et al. 2002; Heldt et al. 2018; Barr et al. 2017). The latter, initially termed "population dormancy" by Judah Folkman in 1972 (Gimbrone et al. 1972) and then renamed to tumour mass dormancy, remains poorly understood due to the lack of suitable data and models (Boire et al. 2019).

The theoretical model of TMD is embedded into the "3Es of immunoediting" paradigm (Dunn, Old, and Schreiber 2004b), arising as a temporary equilibrium between tumour elimination and immune escape (Teng et al. 2008; Koebel et al. 2007). As the cancer lesion develops, a period of immunoediting follows when the immune system interacts with the malignant cells establishing a dynamic equilibrium: the immunogenic cells are eliminated, and non-immunogenic tumour cells arise (Dunn, Old, and Schreiber 2004a). This keeps the tumour in a dormant state (H.F. Wang et al. 2019; Aguirre-Ghiso 2007), hypothesised to account for the "latency" between the initiation of the first mutator phenotype and symptom manifestation in early disease, or for the disease-free period preceding cancer recurrence (Gužvić and Klein 2013; Damen, van Rheenen, and Scheele 2020). During this period of dormancy, the continued cytotoxic response triggered by pro-inflammatory signalling cytokines like interferon ɣ, as well as prolonged exposure to pro-inflammatory signalling in general, causes the cytotoxic cells to become inactive, a phenomenon known as T cell exhaustion (Dunn, Koebel, and Schreiber 2006; Wherry and Kurachi 2015; Yi, Cox, and Zajac 2010). Finally, the angiogenic switch or immune escape shifts the balance in favour of cancer progression (Jahanban-Esfahlan et al. 2019).

A variety of molecular mechanisms have been proposed to mediate these switches. The urokinase receptor (uPAR) regulates tumour growth by controlling β1 integrin signalling which drives a cascade of Ras/ERK mitogenic activation via the focal adhesion kinase (FAK) and the EGF receptor (EGFR) (Aguirre Ghiso, Kovalski, and Ossowski 1999; White et al. 2004; Liu et al. 2002; Aguirre Ghiso 2002). Downregulation of any of these components has been shown to lead to tumour growth arrest and dormancy (Aguirre-Ghiso 2007). Additionally, blocking uPAR activates p38, which induces dormancy under p53 upregulation and downregulation of JUN (Ranganathan et al. 2006). Metastatic lesions appear to manifest reduced p38 activity under sustained ERK activation. As a result, a low ERK:p38 protein expression ratio is often employed to assess tumour dormancy (Aguirre-Ghiso et al. 2003). This state is further corroborated by a limited ability in recruiting new blood vessels and vasculature remodelling, resulting in angiogenic dormancy (Moserle, Amadori, and Indraccolo 2009). This condition is often characterised by VEGF inhibition in the presence of anti-angiogenic factors such as

angiostatin, endostatin, thrombospondin, etc., or chemokines (CXCL9, CXCL10) (Senft and Ronai 2016; Lyu et al. 2013; Aguirre-Ghiso 2007; Park and Nam 2020).

Overall, it is clear that TMD results from an interplay between immunological and angiogenic dormancy, where cell growth is counterbalanced by apoptosis due to poor vascularisation and immune cytotoxicity, followed by exhaustion. It becomes evident that the states of T cell exhaustion and dormancy are not a simple dysfunction, but a purposeful homeostatic mechanism enabling the prevention of pathological immune responses. Hence, it is of crucial importance to be able to identify and target the dormant tumours early. This temporary equilibrium state provides a unique clinical opportunity, but its prevalence in cancer and the genetic determinants that may sustain it are currently unknown.

In this study, we surveyed the landscape of TMD along the two axes that shape it, immunological and angiogenic dormancy, in a cohort of 9,631 tumours from 31 tissues available from TCGA. We show that TMD can be captured from bulk sequencing datasets, that it is pervasive across a variety of cancer types and that its emergence is linked with key somatic alterations. We also investigate the environmental context of TMD and its relevance in the clinic.

2 Results

2.1 Pan-cancer characterisation of immunological, angiogenic and tumour mass dormancy

To evaluate the levels of immunological and angiogenic dormancy, as well as immune exhaustion, across multiple cancer tissues, we manually curated lists of genes associated with the three programmes from the literature (Supplementary Table 1). The lists included receptor molecules, as well as soluble mediators, surface and structural proteins, enzymes and transcription factors, several of which are observed to be frequently mutated during cancer development (Supplementary Figure 1). Based on the expression of genes associated with each process, immunological/angiogenic dormancy and exhaustion programme scores were assigned on a per-sample basis (see Materials and Methods, Supplementary Figure 2). Both immunological and angiogenic dormancy represent potential mechanisms for restricting the expansion of primary tumour cell populations due to either impaired vascularization or immunosurveillance (Aguirre-Ghiso 2007), therefore both processes can contribute to the development of TMD. As such, an overall per-patient TMD programme score was also derived using the expression of genes associated with both types of dormancy (Supplementary Figure 2).

Having established a framework for quantifying immunological, angiogenic and tumour mass dormancy programmes, we next profiled these cellular programmes across 9,631 samples of solid primary tumours from the Cancer Genome Atlas (TCGA). We observed a spectrum of TMD across tumours that ranges from highly dormant to highly expanding (Figure 1A-C, Supplementary Figure 3). TMD is thought to emerge when tumour cell proliferation is balanced by apoptosis due to factors such as limitations in blood supply or an active immune system (Holmgren, O'Reilly, and Folkman 1995). Consequently, primary tumour samples with high TMD programme scores (upper quartile of the score range) which also showed a proliferation/apoptosis ratio below 1 (see Materials and Methods), indicative of limited primary tumour lesion expansion, were classed as exhibiting TMD (Figure 1D). Overall, 16.5% of samples across different tissues exhibited substantial evidence for TMD (with up to 33% prevalence in certain cancers) and they were further subdivided into those indicating angiogenic dormancy (4.4%), immunological dormancy (5%), or both (7%) (Figure 1E, Supplementary Figure 4 and Supplementary Table 2). Head and neck (32%), sarcoma (32%) and breast (26%) cancer were among the cancers with highest rates of TMD. Angiogenic dormancy alone was most widespread in breast (14%) and head and neck cancers (13%). Some rarer cancers like thymoma or

127 pheochromocytoma and paraganglioma also showed remarkably high prevalence of TMD (~33% each)
128 with the latter also exhibiting the highest immune-mediated dormancy (21%). The systematic
129 differences in TMD programme scores across different tissues (Figure 1E-F, Supplementary Figure 4)
130 suggest that the tissue environment may impact the ability of the tumour to enter a TMD state. Across
131 the board, immune-mediated dormancy levels appeared higher than those of angiogenic dormancy,
132 suggesting a dominant role for immune surveillance in determining TMD.

133 **2.2 The genomic background of TMD**

134 To gain a better understanding of the genomic context in which TMD can develop, we asked whether
135 samples with high and low TMD differed in their association with known drivers of tumorigenesis. We
136 found 15 genes with either a statistically significant enrichment or a depletion of mutations within
137 samples classed as showing TMD across the 31 solid cancer tissues (Fisher's exact test adjusted
138 $p<0.05$, Figure 2A, Supplementary Table 3). Furthermore, mutations in *MUC4*, a gene involved in
139 angiogenesis and metastasis (Zhi et al. 2014), were specifically enriched in stomach adenocarcinoma,
140 while *EGFR*, *FAT3/4*, *LRP1B*, *KAT6B* mutations, mainly linked with cell proliferation and immune
141 responses (Katoh 2012; H. Chen et al. 2019; Simó-Riudalbas et al. 2015; Sigismund, Avanzato, and
142 Lanzetti 2018), were depleted in colon cancer (Fisher's exact test adjusted $p<0.05$, Supplementary
143 Figure 5). Many of these findings were reaffirmed using a random forest classification approach
144 (Supplementary Figure 6).

145 The results of the pan-cancer analysis largely reflected the balance of proliferation, cell death and
146 pro/anti-angiogenic signals (Naumov et al. 2006; Semenza 2003; Aguirre-Ghiso 2007) one would
147 expect in the context of dormancy. Two genes stood out as having a ~5-fold enrichment of mutations
148 in patients displaying TMD: *HRAS* and *CASP8*. Interestingly, while *HRAS* alterations were positively
149 associated with dormancy, other members of the same oncogenic family, *KRAS* and *NRAS* showed a
150 depletion of mutations in the context of this phenotype. Specifically, we found an enrichment of *HRAS*
151 hotspot mutations at the Q61 and G13 positions across all solid primary tumour samples, but a
152 depletion of *KRAS* G13 and G12, as well as *NRAS* Q61 hotspot alterations (Supplementary Figure 7).
153 The oncogenic activation of the Ras protein has been associated with pro-angiogenic signaling through
154 repression of thrombospondin-1 (Watnick et al. 2015). It has been suggested that while distinct
155 oncogenic Ras alterations might have similar ability to promote cell cycle progression, they might have
156 different abilities to induce the pro-angiogenic programme (Aguirre-Ghiso 2007), which may explain
157 the discrepancy of mutation signals in the *RAS* genes in relation to TMD.

158 *CASP8*, a gene encoding a cysteine-aspartic acid protease involved in the execution of apoptosis by
159 cleaving and thereby activating caspase-3 and caspase-7 (Tummers and Green 2017), was also
160 preferentially mutated in dormancy. While *CASP8* loss of function would be predicted to impair the
161 ability of cancer cells to initiate apoptosis, silencing of *CASP8* in breast cancer cell lines has also been
162 shown to decrease cancer cell growth by delaying G0/G1- to S-phase transition and increasing the
163 expression of CDK inhibitors p21 and p27 (De Blasio et al. 2016).

164 The genes presenting a depletion of point mutations within dormant samples identified by our analysis
165 have key functions in regulating tumour growth, including *TP53*, the master regulator that coordinates
166 signals of stress such as DNA damage and aberrant growth signaling and can induce cell cycle arrest
167 or apoptosis (Vogelstein, Lane, and Levine 2000; Polyak et al. 1997), or *APC*, which suppresses tumour
168 growth through repression of the Wnt signaling pathway (Boman and Fields 2013). Both the *APC* and
169 *DCC* genes promote apoptosis by downregulation of survivin gene expression (Zhang et al. 2001) and
170 caspase-9 cleavage (Forcet et al. 2001) respectively. Control of tumour vascularization was reflected

171 in depletion of mutations in *PRDM16*, which inhibits angiogenesis by suppressing the expression of a
172 HIF target semaphorin 5B (Kundu et al. 2020), and in *NCO1A*, a transcriptional coactivator that
173 upregulates the expression of the VEGFα pro-angiogenic factor (Qin et al. 2015). Mutations in the
174 *IDH1* gene, shown to be depleted in samples with TMD, result in the production of the 2-
175 hydroxyglutarate metabolite which regulates the activity of α-ketoglutarate dependent dioxygenases
176 and causes the ubiquitination and proteasomal degradation of *HIF1A*, a key sensor of hypoxia and
177 initiator of angiogenesis (Ye et al. 2013). Moreover, 2-hydroxyglutarate can also result in the
178 downregulation of leukocyte chemotaxis factors (Turcan et al. 2012; Tommasini-Ghelfi et al. 2019),
179 which could contribute to the ability of tumour cells to escape immunological dormancy through
180 immune system evasion.

181 In addition to the enrichment analysis, using a maximum-likelihood dN/dS method (Martincorena et
182 al. 2017) we detected signals of positive selection for mutations within *CASP8* and *HRAS* in samples
183 with TMD, but not in expanding tumour samples (Figure 2B). In contrast, *IDH1* and *NRAS*, both of
184 which showed a depletion of mutations within TMD samples, showed signals of positive selection only
185 in expanding tumours (Figure 2B). These findings support the importance of *CASP8*, *HRAS*, *NRAS* and
186 *IDH1* mutational status in the context of TMD.

187 In terms of broader structural variation in the genome, we found no copy number alteration events
188 (amplifications and deletions) specifically enriched in tumours with TMD (data not shown), potentially
189 because such events would be preferentially selected for in fast growing tumours. Moreover, tumours
190 with angiogenic and immunological dormancy showed a modest, but significant decrease in mutational
191 burden when compared to tumours without TMD (Supplementary Figure 8).

192 **2.3 Mutational processes linked with dormancy and exhaustion**

193 In addition to investigating the links with specific driver events, we also set out to characterise broader
194 mutational processes associated with TMD. Different risk factors of cancer induce DNA damage in the
195 cells in a context dependent manner, such that nucleotide substitution patterns associated with various
196 such mutational processes can be observed within cancer genomes. These patterns of trinucleotide
197 substitutions are termed "mutational signatures" and have been widely characterised across cancers
198 (Alexandrov, Nik-Zainal, Wedge, Aparicio, et al. 2013; Alexandrov et al. 2020). We carried out
199 mutational signature analysis to survey the contribution of known mutagenic processes and risk factors
200 to the genomes of dormant tumours. The mutational signature prevalence was correlated with
201 dormancy and exhaustion programme scores (Figure 2C, left and centre panels).

202 We observed that exposure to signatures SBS1 and 5, originating from aging-induced deamination of
203 5-methylcytosines (Alexandrov et al. 2015), and SBS22, linked with aristolochic acid exposure
204 (Jelaković et al. 2015), decreased as TMD and exhaustion increased. In contrast, smoking (SBS4) and
205 defective base excision repair linked with polymerase epsilon or *NTHL1* mutations (SBS10a/b, SBS30)
206 (Jager et al. 2019; Shivji et al. 1995) were associated with an increase in TMD. Finally, we noted a
207 consistently strong correlation between TMD/exhaustion and mutational signatures SBS2 and SBS13,
208 associated with mutagenesis induced by a class of cytidine deaminases called APOBEC
209 (apolipoprotein B mRNA editing catalytic polypeptide-like) (Alexandrov et al. 2020). These enzymes
210 induce mutagenesis in viral genetic material and are part of anti-viral defence, but can also act on and
211 damage host DNA (Green and Weitzman 2019). The correlation of these mutational footprints of
212 APOBEC with TMD was observed both pan-cancer and across individual cancer types, including
213 bladder, breast, cervical and head and neck cancers (Figure 2C). Reassuringly, there was a similarly

214 strong correlation between SBS2 and SBS13 and the mean expression of the AID/APOBEC cytidine
215 deaminases (Figure 2C, right panel).

216 **2.4 Dormancy and exhaustion programmes correlate with APOBEC enzymatic activity**

217 To further explore the association between TMD and exhaustion with APOBEC mutagenesis, we
218 calculated the correlation of our programme scores and the mean expression of genes belonging to the
219 APOBEC family (Figure 3A-F). Across all cancers, we observed significant correlations between the
220 activity of the APOBEC programme as a whole, TMD and exhaustion programmes (Figure 3 A-G). In
221 particular, we observed a marked association between APOBEC mutagenesis and immunological
222 dormancy, which we stipulate may precede or come in conjunction with immune exhaustion, the latter
223 showing the strongest correlation.

224 We also observed positive correlations between most but not all genes included in the immunological,
225 angiogenic and exhaustion programmes, on the one side, and the expression of the AID/APOBEC
226 enzyme family members, on the other (Figure 3H). This may be because of downstream regulation of
227 expression, e.g. through mRNA degradation, compartmentalization, or inhibition of transcription.
228 Notably, among all genes, the correlation was highest for the mRNAs of enzymatically active
229 APOBEC3 and AID members of the APOBEC family. The correlation scores were similar for
230 *APOBEC3A-H*, which is to be expected as these genes form a cluster on chromosome 22. Within the
231 TMD programme, type II interferon ɣ gene and the interferon-upregulated genes such as *STAT1*
232 showed a positive correlation with APOBEC. This is interesting as interferon ɣ signaling is associated
233 with anti-tumour response by favoring rejection of highly immunogenic tumours (Mittal et al. 2014;
234 Benci et al. 2016). However, prolonged interferon ɣ signaling promotes epigenetic changes to *STAT1*
235 and promotes expression of ligands for multiple T cell inhibitory receptors (Benci et al. 2016). Thus,
236 we would expect a spectrum of exhaustion signaling to be present within the tumour, ranging from
237 cells signaling danger to cells with anti-cytotoxic response. Anti-angiogenic markers, such as the
238 urokinase receptor *PLAUR*, which downregulate angiogenic processes and thus restrict the supply of
239 T cells (Oh, Hoover-Plow, and Plow 2003), were also positively correlated with APOBEC expression.
240 Similar associations were observed for several immune checkpoints (*CD244*, *CD166*, *TIGIT*, *CTLA4*,
241 *PDCD1*) and exhaustion markers (*EOMES*, *TBX21*).

242 Overall, the multiple correlations between APOBEC expression and the dormancy/exhaustion levels
243 in tumours suggest a complex interplay between the activity of APOBEC deaminases and the immune
244 microenvironment, which we set out to explore in greater depth.

245 **2.5 TMD activity differences in the context of APOBEC mutagenesis**

246 To further elucidate the association between TMD and APOBEC activity, we sought to investigate the
247 specific TMD signals that might have the strongest links with APOBEC-attributable mutagenesis, as
248 quantified by the single-base substitution mutational signatures SBS2 and SBS13. In order to identify
249 APOBEC-enriched tumours, we employed t-distributed stochastic neighbour embedding (tSNE) to
250 cluster samples based on their overall mutational signature profiles (Figure 4A-B). Unsurprisingly, the
251 clustering was impacted by the tumour tissue of origin, as mutational signatures are often tissue-
252 specific (Degasperi et al. 2020) (Figure 4A). However, samples enriched for APOBEC-associated
253 mutations, defined as the total enrichment of signatures SBS2 and SBS13, covered a fairly
254 heterogenous set of tissues (Figure 4B). Groups with distinct mutagenesis patterns were defined using
255 expectation-maximization clustering (Supplementary Figure 9), and the procedure was repeated 100
256 times to obtain robust clusters. Samples were defined as APOBEC-enriched if they fell into the
257 APOBEC-associated cluster more than 50 times (see Materials and Methods), which broadly overlaps

258 with the APOBEC enrichment score approach developed by Roberts et al (Roberts et al. 2013)
259 (Supplementary Figure 10).

260 To determine whether APOBEC mutagenesis was specifically associated with particular aspects of the
261 TMD programme, we used random forest classifiers to rank TMD genes based on how much their
262 expression helps to distinguish between the APOBEC-enriched and depleted groups (see Materials and
263 Methods). The accuracies for predicting APOBEC enrichment across 100 built models were
264 remarkably high and broadly replicable (mean AUC = 0.8354, range: 0.8203-0.8534) (Figure 4C-D).
265 Additionally, the gene ranking in the models was also highly reproducible (Figure 4E). *PLG*, which
266 encodes for the plasminogen protein and triggers angiostatin release to inhibit angiogenesis (Oh,
267 Hoover-Plow, and Plow 2003), displayed the highest importance by far, defined as the mean associated
268 decrease in Gini index following its removal from a model (mean = 119.2). Upon further investigation
269 of *PLG* expression, we found that its high predictive importance could largely be attributed to a
270 substantial group of low-*PLG*-expressing samples which were not labelled as APOBEC-enriched
271 (Figure 4F). This becomes more apparent when considering the multidimensional scaling plot
272 attributable to one of the random forest classifiers, which clearly displays a segregated cluster of non-
273 APOBEC-enriched samples defined by a specific *PLG* expression threshold derived from the classifier
274 (Figure 4G). Therefore, APOBEC mutagenesis appears to be completely lacking in the cases when
275 *PLG* is not expressed, suggesting a link between APOBEC enzymatic activity and the uPA/uPAR
276 system of angiogenic modulation.

277 Finally, we compared the expression of genes associated with TMD between APOBEC mutagenesis
278 enriched and depleted groups. The large majority of genes whose upregulation drives TMD displayed
279 a higher median expression in APOBEC-enriched samples compared with non-enriched samples
280 (Figure 4H). It is worth noting that some genes were found to be significantly changed whilst
281 displaying negligible difference in medians, likely reflecting the effects of a large sample size rather
282 than a real biological difference. Overall, these results reaffirm the positive correlation between TMD
283 and APOBEC enzyme activity, apparent both from an expression and mutagenesis perspective.

284 **2.6 Heterogeneity of TMD maintenance in hypoxic conditions**

285 Owing to the reported association between hypoxic environments and angiogenesis (L. Chen, Endler,
286 and Shibasaki 2009), we next sought to investigate whether hypoxia might differentially impact TMD.
287 Hypoxia was quantified on a per-sample basis using established transcriptional signatures (see
288 Materials and Methods), and the calculation procedure was validated using three separate hypoxia
289 signatures (Supplementary Figure 11).

290 From a pan-cancer perspective, we observed that hypoxia scores were significantly lower in samples
291 displaying any type of dormancy, compared to samples with no evidence of TMD (Figure 5A). This
292 was further corroborated by grouping tumours into distinct subsets (bins) based on their hypoxia levels:
293 the proportion of samples with no evidence of TMD increased significantly as hypoxia scores increased
294 (Figure 5B). In particular, we noted the lowest hypoxia levels appearing in tumours with angiogenic
295 dormancy. These results align with the established consensus that the hypoxia-inducible factor (HIF)
296 pathway is a key regulator of angiogenesis (Pugh and Ratcliffe 2003; Krock, Skuli, and Simon 2011),
297 with angiogenic dormancy expected to develop in normoxic conditions. Similar patterns were also
298 observed on a tissue-specific basis, particularly in the cases of sarcoma, stomach, lung squamous and
299 esophageal carcinomas (Figure 5C). Cancer studies which tended to present low hypoxia, such as
300 pheochromocytoma and paraganglioma (PCPG), thymoma (THYM) and thyroid carcinoma (THCA)
301 often presented some evidence of TMD, whereas studies presenting high hypoxia, such as colon and

302 rectum adenocarcinomas (COAD/READ) and glioblastoma (GBM), were abundant in expanding
303 tumours (Supplementary Figure 12). Notable exceptions included bladder cancer and uveal melanoma,
304 both of which presented samples with evidence of TMD at the higher end of their respective hypoxia
305 spectra (Figure 5C-F). While prior research has highlighted HIF1 alpha expression as a promoter of
306 angiogenesis and tumour invasion in bladder carcinoma (Theodoropoulos et al. 2004) and metastasis
307 in uveal melanoma (Asnaghi et al. 2014), our analysis suggests that a period of TMD-induced latency
308 may also be compatible with hypoxia in these cancers.

309 While a considerable heterogeneity across cancer tissues was observed, patterns of decreased hypoxia
310 in the context of TMD were noted in the majority of cancers (Figure 5D-F). This would imply that
311 hypoxia may be an impediment to TMD maintenance across the majority of tumours, consistent with
312 its increased prevalence in the later stages of tumour development (Petrova et al. 2018).

313 **2.7 The microenvironmental context of TMD**

314 Since TMD is by definition dependent on immune surveillance, we also set out to confirm this and
315 potentially identify new components of the cancer microenvironment which are permissive to this type
316 of dormancy. Specifically, because the balance in the populations of immune and stromal cells is
317 central to forming anti-tumour responses, we investigated how immune composition might be shaped
318 in the context of TMD, exhaustion and APOBEC programmes. Using cell type-specific transcriptional
319 markers (see Materials and Methods), we observed strong positive correlations between TMD and
320 various types of T cells (Figure 6A). Antitumoral cytotoxic cells such as CD8+ and CD4+ T cells,
321 Th1/2 cells, as well as tumour promoting regulatory cells and macrophages were correlated with the
322 APOBEC, exhaustion and dormancy programmes. This observation is in line with the mechanism
323 proposed in the literature whereby an initial immune response caused by neoantigens presented by the
324 dormant tumours is followed by exhaustion of such signals (Ghorani et al. 2020). In addition to their
325 cytotoxic activity, CD8+ and CD4+ T cells have been previously shown to limit tumour growth through
326 the secretion of anti-proliferative cytokines, such as IFN- γ which can stimulate the expression of p21
327 and p27 cell cycle inhibitors (Wall et al. 2003; Chin et al. 1996), and antiangiogenic chemokines, such
328 as CXCL9 and CXCL10 (Ikeda, Old, and Schreiber 2002).

329 Compared to Th1 and Th2 cells, NK cells showed a weaker correlation with dormancy programmes,
330 consistent with reports of tumour growth control by the immune system being mostly associated with
331 adaptive T cell responses (Finn 2006). The microenvironment of samples with high TMD was also
332 depleted in inflammatory Th17 cells, which secrete the angiogenesis inducer IL-17A (Bailey et al.
333 2014). Interestingly, samples displaying signals of angiogenic dormancy had higher enrichment of Th2
334 instead of Th1 cells. While the Th1 activity is linked with IFN-ɣ production and tumour suppression,
335 Th2 activity has been implicated in cancer progression (Zhao et al. 2019). Despite the broader
336 heterogeneity of T helper cell signals, they showed a similar overall trend as that of cytotoxic and
337 dendritic cells when projected across the TMD landscape (Figure 6B-D). All these classes except for
338 the Th2 cells appeared most enriched in tumours with evidence of both immunological and angiogenic
339 dormancy (Figure 6E).

340 **2.8 TMD is prognostic in cancer**

341 To understand the clinical relevance of TMD, we carried out survival analysis and found that patients
342 with expanding tumours that presented no evidence of TMD had a significantly reduced prognosis
343 (Figure 7A), consistent with the expectation that fast-proliferating tumours should be more aggressive
344 than their dormant counterparts. To further dissect the potential sources of this variation along the
345 immunity/angiogenesis axis, we employed Cox proportional hazards models to determine the effects

346 of different types of dormancy on survival whilst accounting for potential confounders such as patient
347 age, gender, cancer type, and tumour stage. While all three categories were associated with decreased
348 risk when compared to patients with no evidence of TMD, much of this variation was accounted for
349 by tumour stage, with only angiogenic and tumour mass dormancy still marginally significant after
350 correction (Figure 7B, Supplementary Figures 13-17). When comparing the prevalence of TMD
351 between early- and late-stage cancers (Supplementary Figure 18), we found that expanding tumours
352 were, as expected, enriched in late-stage cancers (Fisher's exact test $p < 0.0001$, 1.5-fold enrichment).
353 Surprisingly, samples with angiogenic dormancy were also marginally enriched (1.3-fold) in late-stage
354 cancers (Fisher's exact test $p < 0.05$). While the tumour stage effect may not be fully uncoupled from
355 the TMD effect, TMD did present a marginal protective role within the early-stage tumours (stages
356 I/II), as well as a larger protective role in late-stage tumours (stages III/IV) (Supplementary Figure 19).

357 **3 Discussion**

358 TMD is a key state in tumour development and progression, but its evolutionary constraints are largely
359 unknown. In this study, we have presented an overview of TMD across 31 cancer tissues and
360 highlighted potential novel genomic hallmarks of this state. While TMD remains a poorly characterised
361 programme whose current known markers are undoubtedly incomplete, our approach to evaluating
362 TMD in bulk tumours through an equilibrium of proliferation, apoptosis, cytotoxicity, exhaustion and
363 angiogenesis signals has enabled us to systematically capture this temporary state across a variety of
364 cancers. We show that TMD is present across a multitude of cancer tissues, and that immunological
365 and angiogenic dormancy are not always concomitant. We confirm many of the expected associations
366 reported in the literature, including lower mutational burden, correlations with CD8+, regulatory and
367 helper T cells (Teng et al. 2008), improved prognosis (Park and Nam 2020) and a strong link with
368 immune exhaustion (Mittal et al. 2014). Exhaustion is a phenotype that likely immediately follows
369 TMD, but in our analysis the two states are largely overlapping. This is most likely due to the bulk
370 nature of the samples analysed, where we may be capturing parts of the tumour that starting to expand
371 in addition to areas still displaying TMD. Interestingly, we find TMD tends to occur in normoxic rather
372 than hypoxic environments in the majority of cases, which is different than what is observed for cellular
373 quiescence (Qiu et al. 2017; Butturini et al. 2019).

374 In addition to expected associations, our methodology has also enabled us to capture previously
375 unreported links between multiple mutational processes and TMD. Firstly, we find that oncogenic
376 mutations in *CASP8* (inactivating) and *HRAS* (activating) are positively selected for during the
377 development of TMD. This is either because they might confer an advantage in terms of maintaining
378 TMD, or because they might enable cells to escape TMD and expand further. Interestingly, most of the
379 classical cancer drivers are amplified or deleted preferentially in non-dormant tumours, while TMD
380 appears largely devoid of specific copy number marks. Part of the reason for this may be that TMD
381 often appears in early-stage tumours when these changes have not yet occurred as a means of expansion
382 and escape from immune surveillance. However, we also notice TMD is still evident in a comparable
383 fraction of late-stage tumours (18%) (Supplementary Figure 18). In the absence of longitudinal data
384 that could shed further light into the causes, we can only hypothesise this could be due to a mechanism
385 of slowly advancing cancers that are maintained in a semi-TMD state, potentially enabled by a strong,
386 consistent immune response.

387 In concordance with the reduced rate of cell proliferation in TMD, we find that ageing-induced
388 mutations, which are believed to accumulate at a relatively constant rate in cancer, are lesser
389 represented in dormant tumours. Correlations between TMD and several other mutational processes

390 (smoking, defective DNA repair) were noted, which might suggest that multiple neoplastic
391 mechanisms that are tissue-specific could favour this state.

392 A remarkably consistent signal came from the mutagenesis trace left by the APOBEC enzyme family.
393 APOBEC activity appeared strongly linked with the exhaustion signals that presumably follow TMD,
394 and with immunological dormancy. Several studies (Yamazaki et al. 2019; Swanton et al. 2015; Burns,
395 Temiz, and Harris 2013) have proposed that APOBEC expression may be one of the drivers of
396 tumorigenesis, suggesting a role for APOBECs in evading immune response. APOBEC3 signatures
397 are prevalent in leukaemias (Rebhandl et al. 2014), while AID was demonstrated to induce
398 hypermutation and chromosomal translocation in B cell lymphomas (Robbiani and Nussenzweig
399 2013). On the other hand, APOBEC may promote the formation of neoantigens and activate cytotoxic
400 T cell responses. It was shown that the APOBEC3 class of enzymes is upregulated in immune cells
401 (monocytes, macrophages and pDCs) upon treatment with interferon ɣ (F.X. Wang et al. 2008;
402 Stenglein et al. 2010). In ovarian carcinoma, the expression of APOBEC3G was positively correlated
403 with T cell infiltration, expression of cytotoxic granzyme and perforin (*GZMB*, *PRF1*), and improved
404 clinical outcome (Leonard et al. 2016). Moreover, APOBEC mutagenesis has previously been linked
405 with responses to immunotherapy in lung, melanoma and head and neck cancers (S. Wang et al. 2018;
406 Faden et al. 2019; Driscoll et al. 2020) through the induction of heteroclitic neoepitopes. We have
407 demonstrated increased APOBEC mutagenesis in a TMD setting across multiple tumour types, and
408 have shown that this process appears linked with the regulation of angiogenesis by the uPAR system.
409 It is possible that the mutational footprint left in the genome by such activity enables immune
410 recognition and maintenance of TMD in the time span until exhaustion and immune escape occurs.
411 This could suggest a window of opportunity for the employment of checkpoint inhibitors, possibly in
412 combination with APOBEC inhibitors, in early-stage tumours with TMD.

413 Our pan-cancer analysis unveils a complex interplay between TMD, exhaustion and APOBEC activity,
414 and a mutational context that may enable these phenotypes to develop. It is possible the correlations
415 identified between the dormancy, exhaustion, APOBEC and hypoxia programmes are not the result of
416 direct interactions in the system but rather are the result of a more complex mechanism, where TMD
417 and APOBEC activity are not directly related. Moreover, changes in gene expression may not
418 accurately reflect changes in abundance of protein products in our defined dormancy and exhaustion
419 programmes. Biochemical assays and studies in model organisms will give a more definite answer to
420 the nature of these relationships.

421 An important limitation of this analysis consists in the fact that the samples analysed have been profiled
422 using bulk sequencing methods, which means that we are only capturing an average cellular signal
423 across the entire tumour which may not reflect its true heterogeneity. Furthermore, since TMD is a
424 temporary phenotype, a single static snapshot of tumours, even in this large dataset, may not be
425 sufficient to capture the entire array of TMD phenotypes that might develop in different tissues.
426 Therefore, multi-regional sequencing and longitudinal studies should be conducted in the future to shed
427 further light on the diversity and dynamics of TMD phenotypes.

428 Furthermore, our study focused mainly on pan-cancer markers of TMD, due to the scarcity of this
429 phenotype. From our analyses, we observe TMD is frequent in certain tissues such as head and neck,
430 breast, bone, and has weak evidence or complete absence of signals in others, e.g. chromophobe renal
431 cell carcinoma. Some of the smaller studies from TCGA may be insufficiently powered to capture such
432 signals. Therefore, future studies should focus on an in-depth characterization of TMD in distinct
433 tissues and should be able to pinpoint tissue-specific genomic markers linked to TMD. Finally, the

potential genomic biomarkers of dormancy that we identified need to be confirmed through experimental validation in suitable in vitro/in vivo models of TMD.

Overall, our study provides evidence for TMD, immunological and angiogenic dormancy signals across a variety of cancer types, and highlights key associated intrinsic and extrinsic hallmarks, including *CASP8*/*RAS* dependencies, APOBEC mutagenesis and hypoxia. These findings pave the way for further exploration of the mechanisms underlying TMD emergence, maintenance and exit.

4 Materials and Methods

4.1 Datasets

FPKM normalised RNA-sequencing expression data as well as mutation annotation files aligned against the hg38 genome from the Muse pipeline, were downloaded using the *TCGAbiolinks* R package (Colaprico et al. 2016) for 9,712 primary tumour TCGA samples across 31 solid cancer types. For patients with multiple samples available, one RNA-seq barcode entry was randomly selected for each individual patient resulting in 9,631 total entries. All expression data were log-transformed for downstream analysis.

4.2 Quantifying the dormancy, exhaustion and APOBEC programmes

Mean log-transformed expression values of genes deemed to be associated with a given programme by manual curation of the literature (Supplementary Table 1) were used to produce per-sample programme scores for immunological/dormancy, exhaustion and APOBEC activity. The APOBEC and exhaustion programme scores were calculated by taking the mean expression of genes within the respective programmes, as all genes in the programmes were expected to be upregulated in the respective states. The dormancy programme scores were calculated by subtracting the sum of downregulated genes from the sum of upregulated genes and dividing by the total number of genes within the programme. The proliferation/apoptosis ratio was calculated by dividing the average expression of E2F target genes (including MKI67, a classical proliferation marker (Miller et al. 2018)), obtained from the "HALLMARK_E2F_TARGETS" gene list, by the average expression of genes involved in apoptosis from the "HALLMARK_APOPTOSIS" gene list. Both gene lists are part of the "H: hallmark gene sets" collection deposited at MSigDB.

Samples with high TMD were identified as being within the upper quartile of the TMD programme score range and presenting a ratio of proliferation/apoptosis < 1. Dormant samples were further classified as having immunological and/or angiogenic dormancy based on whether they were in the upper quartile of the angiogenic (AD) and/or immunological dormancy (ID) programme score range, respectively. Samples with no evidence for TMD (expanding tumours, marked as 'NO') were identified as being in the lower quartile of the TMD programme score range and showing a ratio of proliferation/apoptosis > 1. The remaining samples ('MID' category) were classed as having middle levels of expansion with some weak potential evidence of dormancy, but biologically unlikely to be dormant.

4.3 PHATE dimensionality reduction

The *phateR* R package (Moon et al. 2019) was used to perform the dimensionality reduction based on the expression of genes associated with the TMD and exhaustion programmes. A constant seed was used for reproducibility. The *ComBat* function from the *sva* R package (Leek et al. 2012) was used to remove tissue-specific expression patterns from the TCGA RNA-seq data.

475 **4.4 Association between cancer driver mutations and TMD**

476 The COSMIC database (Tate et al. 2019) was used to source a list of 723 known drivers of
477 tumorigenesis (Tiers 1+2). COSMIC genes mutated in at least 1% of samples across all solid primary
478 tumour samples were tested for enrichment or depletion of mutations between samples with high and
479 low TMD using a Fisher's exact test. Only missense, nonsense, nonstop, frameshift deletion/insertion
480 and inframe insertion/deletion mutations were considered in the analysis. For *HRAS*, *KRAS* and *NRAS*,
481 a Fisher's exact test was also performed to test for enrichment or depletion of specific recurrent hotspot
482 mutations, reported by the cBioPortal data hub and based in part on methodology from Chang et al
483 (Chang et al. 2016) and Gao et al (Gao et al. 2017). The analysis was also repeated on a cancer-by-
484 cancer basis, where COSMIC genes mutated in at least 5% of samples within the cancer-specific study
485 sample were tested for enrichment or depletion of mutations with TMD samples. The p-values were
486 corrected using Benjamini-Hochberg (BH) procedure to accommodate for multiple testing.

487 Enrichment analysis was reaffirmed using a random forest classification approach. This was conducted
488 using the *randomForest* R package. A balanced dataset of samples with high and low TMD was
489 generated by utilising all samples with low TMD (n = 657), and randomly sampling an equal number
490 of samples with high TMD (n = 1,154). The resulting random forest consisted of 500 trees, and
491 mutation enrichment was determined by calculating the mean decrease in Gini index between the two
492 groups following the removal of a gene.

493 To identify genes that are positively selected in the context of TMD, we carried out dN/dS analysis
494 separately for high and low TMD samples using the *dNdScv* R package (Martincorena et al. 2017), run
495 with default parameters.

496 **4.5 Mutational signature analysis**

497 Mutational signature contributions were inferred using *deconstructSigs* (Rosenthal et al. 2016) and the
498 choice of signatures was further informed using results from *SigProfiler* (Alexandrov, Nik-Zainal,
499 Wedge, Campbell, et al. 2013). Only samples with at least 50 mutations were employed in the analysis,
500 for a total of 6,410 samples.

501 *SigProfiler* was used to infer mutational signatures from TCGA whole-exome sequencing data. For
502 each TCGA study of interest, input mutational matrices were generated using the
503 *SigProfilerMatrixGeneratorR* function using all samples containing at least 50 mutations and aligning
504 the MAF files to the hg38 genome build. *SigProfilerExtractorR* was used to extract de novo mutational
505 signatures for each cancer type. For each study, the solution with the greatest number of mutational
506 signatures was chosen, for which also the sum of the solution stability (calculated average silhouette
507 coefficient) and minimum stability exceeded 1, and the minimum stability value did not fall below 0.4.
508 For the selected solutions, the identity of the mutational signatures was determined by calculating
509 cosine similarities with COSMIC v3.1 mutational signatures.

510 Mutational signatures from whole-exome sequencing data were also inferred using the *deconstructSigs*
511 R package. MAF files were aligned against the hg38 genome build and the COSMIC v3.1 mutational
512 signatures were employed in the analysis. For each cancer type, the contribution of all signatures within
513 the *deconstructSigs* solution was set to 0, apart from SBS1, SBS5, signatures identified in the
514 corresponding *SigProfiler* solution, as well as signatures which contribute on average at least 5% of
515 mutations across all samples within the *deconstructSigs* solution. For cancer types where *SigProfiler*
516 did not result in a stable solution, the *deconstructSigs* solution was used with the contribution of all

517 signatures set to 0, apart from SBS1, SBS5 as well as signatures which contribute at least 5% of
518 mutations across samples within the *deconstructSigs* solution.

519 **4.6 Tumour microenvironment deconvolution from bulk RNA-seq data**

520 The tumour microenvironment cell infiltration scores were calculated using the *ConsensusTME* R
521 package (Jiménez-Sánchez, Cast, and Miller 2019) based on gene sets from Bindea et al (Bindea et al.
522 2013). Cell abundance was estimated from the TCGA bulk RNA-seq data using singe sample Gene Set
523 Enrichment Analysis (ssGSEA). Broader categories (cytotoxic cells, Th cells, dendritic cells) were
524 scored by combining the expression across subtype-specific markers.

525 **4.7 Identification of APOBEC mutagenesis clusters**

526 First, APOBEC enrichment scores were calculated using the *sigminer* R package (Shixiang Wang et
527 al. 2020). Next, the mutational signature profiles of 6,410 samples underwent dimensionality reduction
528 with tSNE using the *Rtsne* R package, followed by expectation-maximization clustering using the
529 *EMCluster* R package. The optimal number of clusters was determined by considering the associated
530 increase in log-likelihood pertaining to additional clusters and was assumed to be equivalent for all
531 applications of tSNE (Supplementary Figure 9A). Whilst substantial increases were associated with
532 both 10 and 17 clusters, we selected 10 clusters in order to prevent the cluster of APOBEC-enriched
533 samples from being segmented. The APOBEC-enriched cluster was identified as the cluster with the
534 highest median collective enrichment of APOBEC signatures SBS2 and SBS13. The procedure was
535 conducted 100 times and samples which appeared in the APOBEC-enriched cluster on more than 50
536 occasions were labelled as 'APOBEC enriched'.

537 **4.8 Random forest modelling of APOBEC mutagenesis-gene expression associations**

538 Z-score normalisation of RNA-sequencing expression data was applied across each cancer type
539 individually. The FPKM-normalised values were log-transformed, and the results for each gene were
540 transformed into a $Z \sim N(0,1)$ distribution using the scale function in R. Only genes involved in the
541 dormancy and exhaustion programmes were considered as input in the classifier.

542 Genes whose expression contributed to APOBEC enrichment classification were identified using
543 machine learning via a random forest approach, conducted using the *randomForest* R package. In total,
544 5,850 samples were included for which Z-scores and mutational signature profiles were available. Each
545 random forest model required all samples labelled as APOBEC-enriched ($n = 952$), and an equal
546 number of samples taken randomly without replacement from the non-APOBEC-enriched samples to
547 generate balanced groups. Each random forest consisted of 1,000 trees. The importance of each gene
548 in the model, measured as the associated mean decrease in Gini index following its removal, was also
549 calculated. This procedure was run 100 times.

550 Changes in median gene expression between the APOBEC enriched and non-enriched groups (Figure
551 4H) were determined using a two-sample Wilcoxon rank-sum test. P-values were corrected for multiple
552 testing using the Benjamini-Hochberg procedure.

553 **4.9 Calculation of hypoxia scores**

554 Hypoxia scores were calculated using three transcription-based hypoxia signatures referred to as Buffa
555 (Buffa et al. 2010), West (Eustace et al. 2013) and Winter (Winter et al. 2007), following the calculation
556 procedure detailed by Bhandari et al (Bhandari et al. 2019). Genes which were included in the curated
557 dormancy or exhaustion signatures were subsequently removed from the respective hypoxia signature.

558 Scores were calculated based on the pan-cancer cohort to enable variation in hypoxia between cancer
559 types to be identified. Since we observed a high degree of agreement between the three signatures
560 (Supplementary Figure 11), the Buffa signature was employed in the downstream analysis on account
561 of its use as a reference by Bhandari et al. A binning approach with a window size of 10 was employed
562 to further subdivide tumours into discrete subgroups with increasing levels of hypoxia.

563 **4.10 Survival Analysis**

564 Survival analysis was conducted via the *survival* R package. Hazard ratios were calculated using Cox
565 proportional hazards models and were displayed using the *finalfit* R package. Survival curves were
566 calculated using the Kaplan-Meier formula, and plotted using the *survminer* R package.

567 **4.11 Statistics**

568 Pairwise correlations were calculated using the Pearson correlation statistics. The *corrplot* R package
569 was used to carry out statistical analysis and visualise the correlation matrices. Groups were compared
570 using the Student's t test, Wilcoxon rank-sum test or Kruskal-Wallis test as appropriate. Multiple
571 testing correction was applied using the Benjamini-Hochberg method. The significance threshold was
572 taken as $p < 0.05$.

573 **4.12 Code**

574 All code developed for the purpose of this analysis can be found at the following repository:
575 https://github.com/secrierlab/tumourMassDormancy/tree/v1.0

576 **5 Conflict of Interest**

577 The authors declare that the research was conducted in the absence of any commercial or financial
578 relationships that could be construed as a potential conflict of interest.

579 **6 Author Contributions**

580 MS designed and supervised the study. AJW, DHJ and WL performed the analyses. All authors wrote
581 and approved the manuscript.

582 **7 Funding**

583 AJW and DHJ were supported by MRC DTP grants (MR/N013867/1 and MR/N013867/1,
584 respectively). MS was supported by a UKRI Future Leaders Fellowship (MR/T042184/1), an Academy
585 of Medical Sciences Springboard Award (SBF004\1042) and a Wellcome Trust Seed Award in Science
586 (215296/Z/19/Z).

587 **8 Data Availability Statement**

588 The results published here are based upon data generated by the TCGA Research Network:
589 https://www.cancer.gov/tcga.

590

591

9 References

Aguirre Ghiso, J. A. 2002. "Inhibition of FAK signaling activated by urokinase receptor induces dormancy in human carcinoma cells in vivo." *Oncogene* 21 (16): 2513-24. https://doi.org/10.1038/sj.onc.1205342. https://www.ncbi.nlm.nih.gov/pubmed/11971186.

Aguirre Ghiso, J. A., K. Kovalski, and L. Ossowski. 1999. "Tumor dormancy induced by downregulation of urokinase receptor in human carcinoma involves integrin and MAPK signaling." *J Cell Biol* 147 (1): 89-104. https://doi.org/10.1083/jcb.147.1.89. https://www.ncbi.nlm.nih.gov/pubmed/10508858.

Aguirre-Ghiso, J. A. 2007. "Models, mechanisms and clinical evidence for cancer dormancy." *Nat Rev Cancer* 7 (11): 834-46. https://doi.org/10.1038/nrc2256. https://www.ncbi.nlm.nih.gov/pubmed/17957189.

Aguirre-Ghiso, J. A., Y. Estrada, D. Liu, and L. Ossowski. 2003. "ERK(MAPK) activity as a determinant of tumor growth and dormancy; regulation by p38(SAPK)." *Cancer Res* 63 (7): 1684-95. https://www.ncbi.nlm.nih.gov/pubmed/12670923.

Alexandrov, L. B., P. H. Jones, D. C. Wedge, J. E. Sale, P. J. Campbell, S. Nik-Zainal, and M. R. Stratton. 2015. "Clock-like mutational processes in human somatic cells." *Nat Genet* 47 (12): 1402-7. https://doi.org/10.1038/ng.3441. https://www.ncbi.nlm.nih.gov/pubmed/26551669.

Alexandrov, L. B., J. Kim, N. J. Haradhvala, M. N. Huang, A. W. Tian Ng, Y. Wu, A. Boot, K. R. Covington, D. A. Gordenin, E. N. Bergstrom, S. M. A. Islam, N. Lopez-Bigas, L. J. Klimczak, J. R. McPherson, S. Morganella, R. Sabarinathan, D. A. Wheeler, V. Mustonen, G. Getz, S. G. Rozen, M. R. Stratton, PCAWG Mutational Signatures Working Group, and PCAWG Consortium. 2020. "The repertoire of mutational signatures in human cancer." *Nature* 578 (7793): 94-101. https://doi.org/10.1038/s41586-020-1943-3. https://www.ncbi.nlm.nih.gov/pubmed/32025018.

Alexandrov, L. B., S. Nik-Zainal, D. C. Wedge, S. A. Aparicio, S. Behjati, A. V. Biankin, G. R. Bignell, N. Bolli, A. Borg, A. L. Børresen-Dale, S. Boyault, B. Burkhardt, A. P. Butler, C. Caldas, H. R. Davies, C. Desmedt, R. Eils, J. E. Eyfjörd, J. A. Foekens, M. Greaves, F. Hosoda, B. Hutter, T. Ilicic, S. Imbeaud, M. Imielinski, M. Imielinsk, N. Jäger, D. T. Jones, D. Jones, S. Knappskog, M. Kool, S. R. Lakhani, C. López-Otín, S. Martin, N. C. Munshi, H. Nakamura, P. A. Northcott, M. Pajic, E. Papaemmanuil, A. Paradiso, J. V. Pearson, X. S. Puente, K. Raine, M. Ramakrishna, A. L. Richardson, J. Richter, P. Rosenstiel, M. Schlesner, T. N. Schumacher, P. N. Span, J. W. Teague, Y. Totoki, A. N. Tutt, R. Valdés-Mas, M. M. van Buuren, L. van 't Veer, A. Vincent-Salomon, N. Waddell, L. R. Yates, J. Zucman-Rossi, P. A. Futreal, U. McDermott, P. Lichter, M. Meyerson, S. M. Grimmond, R. Siebert, E. Campo, T. Shibata, S. M. Pfister, P. J. Campbell, M. R. Stratton, Australian Pancreatic Cancer Genome Initiative, ICGC Breast Cancer Consortium, ICGC MMML-Seq Consortium, and ICGC PedBrain. 2013. "Signatures of mutational processes in human cancer." *Nature* 500 (7463): 415-21. https://doi.org/10.1038/nature12477. https://www.ncbi.nlm.nih.gov/pubmed/23945592.

Alexandrov, L. B., S. Nik-Zainal, D. C. Wedge, P. J. Campbell, and M. R. Stratton. 2013. "Deciphering signatures of mutational processes operative in human cancer." *Cell Rep* 3 (1): 246-59. https://doi.org/10.1016/j.celrep.2012.12.008. https://www.ncbi.nlm.nih.gov/pubmed/23318258.

635 Asnaghi, L., M. H. Lin, K. S. Lim, K. J. Lim, A. Tripathy, M. Wendeborn, S. L. Merbs, J. T. Handa,
636 A. Sodhi, E. E. Bar, and C. G. Eberhart. 2014. "Hypoxia promotes uveal melanoma invasion
637 through enhanced Notch and MAPK activation." *PLoS One* 9 (8): e105372.
638 https://doi.org/10.1371/journal.pone.0105372.
639 https://www.ncbi.nlm.nih.gov/pubmed/25166211.

640 Bailey, S. R., M. H. Nelson, R. A. Himes, Z. Li, S. Mehrotra, and C. M. Paulos. 2014. "Th17 cells in
641 cancer: the ultimate identity crisis." *Front Immunol* 5: 276.
642 https://doi.org/10.3389/fimmu.2014.00276. https://www.ncbi.nlm.nih.gov/pubmed/24987392.

643 Barr, A. R., S. Cooper, F. S. Heldt, F. Butera, H. Stoy, J. Mansfeld, B. Novák, and C. Bakal. 2017.
644 "DNA damage during S-phase mediates the proliferation-quiescence decision in the
645 subsequent G1 via p21 expression." *Nat Commun* 8: 14728.
646 https://doi.org/10.1038/ncomms14728. https://www.ncbi.nlm.nih.gov/pubmed/28317845.

647 Benci, J. L., B. Xu, Y. Qiu, T. J. Wu, H. Dada, C. Twyman-Saint Victor, L. Cucolo, D. S. M. Lee, K.
648 E. Pauken, A. C. Huang, T. C. Gangadhar, R. K. Amaravadi, L. M. Schuchter, M. D.
649 Feldman, H. Ishwaran, R. H. Vonderheide, A. Maity, E. J. Wherry, and A. J. Minn. 2016.
650 "Tumor Interferon Signaling Regulates a Multigenic Resistance Program to Immune
651 Checkpoint Blockade." *Cell* 167 (6): 1540-1554.e12.
652 https://doi.org/10.1016/j.cell.2016.11.022. https://www.ncbi.nlm.nih.gov/pubmed/27912061.

653 Bhandari, V., C. Hoey, L. Y. Liu, E. Lalonde, J. Ray, J. Livingstone, R. Lesurf, Y. J. Shiah, T.
654 Vujcic, X. Huang, S. M. G. Espiritu, L. E. Heisler, F. Yousif, V. Huang, T. N. Yamaguchi, C.
655 Q. Yao, V. Y. Sabelnykova, M. Fraser, M. L. K. Chua, T. van der Kwast, S. K. Liu, P. C.
656 Boutros, and R. G. Bristow. 2019. "Molecular landmarks of tumor hypoxia across cancer
657 types." *Nat Genet* 51 (2): 308-318. https://doi.org/10.1038/s41588-018-0318-2.
658 https://www.ncbi.nlm.nih.gov/pubmed/30643250.

659 Bindea, G., B. Mlecnik, M. Tosolini, A. Kirilovsky, M. Waldner, A. C. Obenauf, H. Angell, T.
660 Fredriksen, L. Lafontaine, A. Berger, P. Bruneval, W. H. Fridman, C. Becker, F. Pagès, M. R.
661 Speicher, Z. Trajanoski, and J. Galon. 2013. "Spatiotemporal dynamics of intratumoral
662 immune cells reveal the immune landscape in human cancer." *Immunity* 39 (4): 782-95.
663 https://doi.org/10.1016/j.immuni.2013.10.003.
664 https://www.ncbi.nlm.nih.gov/pubmed/24138885.

665 Boire, A., S. B. Coffelt, S. A. Quezada, M. G. Vander Heiden, and A. T. Weeraratna. 2019. "Tumour
666 Dormancy and Reawakening: Opportunities and Challenges." *Trends Cancer* 5 (12): 762-765.
667 https://doi.org/10.1016/j.trecan.2019.10.010.
668 https://www.ncbi.nlm.nih.gov/pubmed/31813453.

669 Boman, B. M., and J. Z. Fields. 2013. "An APC:WNT Counter-Current-Like Mechanism Regulates
670 Cell Division Along the Human Colonic Crypt Axis: A Mechanism That Explains How APC
671 Mutations Induce Proliferative Abnormalities That Drive Colon Cancer Development." *Front*
672 *Oncol* 3: 244. https://doi.org/10.3389/fonc.2013.00244.
673 https://www.ncbi.nlm.nih.gov/pubmed/24224156.

674 Buffa, F. M., A. L. Harris, C. M. West, and C. J. Miller. 2010. "Large meta-analysis of multiple
675 cancers reveals a common, compact and highly prognostic hypoxia metagene." *Br J Cancer*
676 102 (2): 428-35. https://doi.org/10.1038/sj.bjc.6605450.
677 https://www.ncbi.nlm.nih.gov/pubmed/20087356.

678 Burns, M. B., N. A. Temiz, and R. S. Harris. 2013. "Evidence for APOBEC3B mutagenesis in
679 multiple human cancers." *Nat Genet* 45 (9): 977-83. https://doi.org/10.1038/ng.2701.
680 https://www.ncbi.nlm.nih.gov/pubmed/23852168.

681 Butturini, E., A. Carcereri de Prati, D. Boriero, and S. Mariotto. 2019. "Tumor Dormancy and
682 Interplay with Hypoxic Tumor Microenvironment." *Int J Mol Sci* 20 (17).
683 https://doi.org/10.3390/ijms20174305. https://www.ncbi.nlm.nih.gov/pubmed/31484342.

684 Chang, M. T., S. Asthana, S. P. Gao, B. H. Lee, J. S. Chapman, C. Kandoth, J. Gao, N. D. Socci, D.
685 B. Solit, A. B. Olshen, N. Schultz, and B. S. Taylor. 2016. "Identifying recurrent mutations in
686 cancer reveals widespread lineage diversity and mutational specificity." *Nat Biotechnol* 34
687 (2): 155-63. https://doi.org/10.1038/nbt.3391.
688 https://www.ncbi.nlm.nih.gov/pubmed/26619011.

689 Chen, H., W. Chong, Q. Wu, Y. Yao, M. Mao, and X. Wang. 2019. "Association of." *Front Immunol*
690 10: 1113. https://doi.org/10.3389/fimmu.2019.01113.
691 https://www.ncbi.nlm.nih.gov/pubmed/31164891.

692 Chen, L., A. Endler, and F. Shibasaki. 2009. "Hypoxia and angiogenesis: regulation of hypoxia-
693 inducible factors via novel binding factors." *Exp Mol Med* 41 (12): 849-57.
694 https://doi.org/10.3858/emm.2009.41.12.103.
695 https://www.ncbi.nlm.nih.gov/pubmed/19942820.

696 Chin, Y. E., M. Kitagawa, W. C. Su, Z. H. You, Y. Iwamoto, and X. Y. Fu. 1996. "Cell growth arrest
697 and induction of cyclin-dependent kinase inhibitor p21 WAF1/CIP1 mediated by STAT1."
698 *Science* 272 (5262): 719-22. https://doi.org/10.1126/science.272.5262.719.
699 https://www.ncbi.nlm.nih.gov/pubmed/8614832.

700 Colaprico, A., T. C. Silva, C. Olsen, L. Garofano, C. Cava, D. Garolini, T. S. Sabedot, T. M. Malta,
701 S. M. Pagnotta, I. Castiglioni, M. Ceccarelli, G. Bontempi, and H. Noushmehr. 2016.
702 "TCGAbiolinks: an R/Bioconductor package for integrative analysis of TCGA data." *Nucleic*
703 *Acids Res* 44 (8): e71. https://doi.org/10.1093/nar/gkv1507.
704 https://www.ncbi.nlm.nih.gov/pubmed/26704973.

705 Damen, M. P. F., J. van Rheenen, and C. L. G.J Scheele. 2020. "Targeting dormant tumor cells to
706 prevent cancer recurrence." *FEBS J*. https://doi.org/10.1111/febs.15626.
707 https://www.ncbi.nlm.nih.gov/pubmed/33190412.

708 De Blasio, A., R. Di Fiore, M. Morreale, D. Carlisi, R. Drago-Ferrante, M. Montalbano, C. Scerri, G.
709 Tesoriere, and R. Vento. 2016. "Unusual roles of caspase-8 in triple-negative breast cancer
710 cell line MDA-MB-231." *Int J Oncol* 48 (6): 2339-48. https://doi.org/10.3892/ijo.2016.3474.
711 https://www.ncbi.nlm.nih.gov/pubmed/27082853.

712 Degasperi, A., T. D. Amarante, J. Czarnecki, S. Shooter, X. Zou, D. Glodzik, S. Morganella, A. S.
713 Nanda, C. Badja, G. Koh, S. E. Momen, I. Georgakopoulos-Soares, J. M. L. Dias, J. Young,
714 Y. Memari, H. Davies, and S. Nik-Zainal. 2020. "A practical framework and online tool for
715 mutational signature analyses show inter-tissue variation and driver dependencies." *Nat*
716 *Cancer* 1 (2): 249-263. https://doi.org/10.1038/s43018-020-0027-5.
717 https://www.ncbi.nlm.nih.gov/pubmed/32118208.

718 Driscoll, C. B., M. R. Schuelke, T. Kottke, J. M. Thompson, P. Wongthida, J. M. Tonne, A. L. Huff,
719 A. Miller, K. G. Shim, A. Molan, C. Wetmore, P. Selby, A. Samson, K. Harrington, H.
720 Pandha, A. Melcher, J. S. Pulido, R. Harris, L. Evgin, and R. G. Vile. 2020. "APOBEC3B-
721 mediated corruption of the tumor cell immunopeptidome induces heteroclitic neoepitopes for

722 cancer immunotherapy." *Nat Commun* 11 (1): 790. https://doi.org/10.1038/s41467-020-
723 14568-7. https://www.ncbi.nlm.nih.gov/pubmed/32034147.

724 Dunn, G. P., C. M. Koebel, and R. D. Schreiber. 2006. "Interferons, immunity and cancer
725 immunoediting." *Nat Rev Immunol* 6 (11): 836-48. https://doi.org/10.1038/nri1961.
726 https://www.ncbi.nlm.nih.gov/pubmed/17063185.

727 Dunn, G. P., L. J. Old, and R. D. Schreiber. 2004a. "The immunobiology of cancer
728 immunosurveillance and immunoediting." *Immunity* 21 (2): 137-48.
729 https://doi.org/10.1016/j.immuni.2004.07.017.
730 https://www.ncbi.nlm.nih.gov/pubmed/15308095.

731 ---. 2004b. "The three Es of cancer immunoediting." *Annu Rev Immunol* 22: 329-60.
732 https://doi.org/10.1146/annurev.immunol.22.012703.104803.
733 https://www.ncbi.nlm.nih.gov/pubmed/15032581.

734 Eustace, A., N. Mani, P. N. Span, J. J. Irlam, J. Taylor, G. N. Betts, H. Denley, C. J. Miller, J. J.
735 Homer, A. M. Rojas, P. J. Hoskin, F. M. Buffa, A. L. Harris, J. H. Kaanders, and C. M. West.
736 2013. "A 26-gene hypoxia signature predicts benefit from hypoxia-modifying therapy in
737 laryngeal cancer but not bladder cancer." *Clin Cancer Res* 19 (17): 4879-88.
738 https://doi.org/10.1158/1078-0432.CCR-13-0542.
739 https://www.ncbi.nlm.nih.gov/pubmed/23820108.

740 Faden, D. L., F. Ding, Y. Lin, S. Zhai, F. Kuo, T. A. Chan, L. G. Morris, and R. L. Ferris. 2019.
741 "APOBEC mutagenesis is tightly linked to the immune landscape and immunotherapy
742 biomarkers in head and neck squamous cell carcinoma." *Oral Oncol* 96: 140-147.
743 https://doi.org/10.1016/j.oraloncology.2019.07.020.
744 https://www.ncbi.nlm.nih.gov/pubmed/31422205.

745 Finn, O. J. 2006. "Human tumor antigens, immunosurveillance, and cancer vaccines." *Immunol Res*
746 36 (1-3): 73-82. https://doi.org/10.1385/IR:36:1:73.
747 https://www.ncbi.nlm.nih.gov/pubmed/17337768.

748 Forcet, C., X. Ye, L. Granger, V. Corset, H. Shin, D. E. Bredesen, and P. Mehlen. 2001. "The
749 dependence receptor DCC (deleted in colorectal cancer) defines an alternative mechanism for
750 caspase activation." *Proc Natl Acad Sci U S A* 98 (6): 3416-21.
751 https://doi.org/10.1073/pnas.051378298. https://www.ncbi.nlm.nih.gov/pubmed/11248093.

752 Gao, J., M. T. Chang, H. C. Johnsen, S. P. Gao, B. E. Sylvester, S. O. Sumer, H. Zhang, D. B. Solit,
753 B. S. Taylor, N. Schultz, and C. Sander. 2017. "3D clusters of somatic mutations in cancer
754 reveal numerous rare mutations as functional targets." *Genome Med* 9 (1): 4.
755 https://doi.org/10.1186/s13073-016-0393-x.
756 https://www.ncbi.nlm.nih.gov/pubmed/28115009.

757 Gerlinger, M., N. McGranahan, S. M. Dewhurst, R. A. Burrell, I. Tomlinson, and C. Swanton. 2014.
758 "Cancer: evolution within a lifetime." *Annu Rev Genet* 48: 215-36.
759 https://doi.org/10.1146/annurev-genet-120213-092314.
760 https://www.ncbi.nlm.nih.gov/pubmed/25292359.

761 Ghorani, E., J. L. Reading, J. Y. Henry, M. R. de Massy, R. Rosenthal, V. Turati, K. Joshi, A. J. S.
762 Furness, A. B. Aissa, S. K. Saini, S. Ramskov, A. Georgiou, M. W. Sunderland, Y. N. S.
763 Wong, M. V. De Mucha, W. Day, F. Galvez-Cancino, P. D. Becker, I. Uddin, M. Ismail, T.
764 Ronel, A. Woolston, M. Jamal-Hanjani, S. Veeriah, N. J. Birkbak, G. A. Wilson, K.
765 Litchfield, L. Conde, J. A. Guerra-Assunção, K. Blighe, D. Biswas, R. Salgado, T. Lund, M.

766 Al Bakir, D. A. Moore, C. T. Hiley, S. Loi, Y. Sun, Y. Yuan, K. AbdulJabbar, S. Turajilic, J.
767 Herrero, T. Enver, S. R. Hadrup, A. Hackshaw, K. S. Peggs, N. McGranahan, B. Chain, C.
768 Swanton, and S. A. Quezada. 2020. "The T cell differentiation landscape is shaped by tumour
769 mutations in lung cancer." *Nat Cancer* 1 (5): 546-561. https://doi.org/10.1038/s43018-020-
770 0066-y. https://www.ncbi.nlm.nih.gov/pubmed/32803172.

771 Gimbrone, M. A., S. B. Leapman, R. S. Cotran, and J. Folkman. 1972. "Tumor dormancy in vivo by
772 prevention of neovascularization." *J Exp Med* 136 (2): 261-76.
773 https://doi.org/10.1084/jem.136.2.261. https://www.ncbi.nlm.nih.gov/pubmed/5043412.

774 Green, A. M., and M. D. Weitzman. 2019. "The spectrum of APOBEC3 activity: From anti-viral
775 agents to anti-cancer opportunities." *DNA Repair (Amst)* 83: 102700.
776 https://doi.org/10.1016/j.dnarep.2019.102700.
777 https://www.ncbi.nlm.nih.gov/pubmed/31563041.

778 Gužvić, M., and C. A. Klein. 2013. "Cancer dormancy: time to explore its clinical relevance." *Breast*
779 *Cancer Res* 15 (6): 321. https://doi.org/10.1186/bcr3590.
780 https://www.ncbi.nlm.nih.gov/pubmed/24359585.

781 HADFIELD, G. 1954. "The dormant cancer cell." *Br Med J* 2 (4888): 607-10.
782 https://doi.org/10.1136/bmj.2.4888.607. https://www.ncbi.nlm.nih.gov/pubmed/13190204.

783 Heldt, F. S., A. R. Barr, S. Cooper, C. Bakal, and B. Novák. 2018. "A comprehensive model for the
784 proliferation-quiescence decision in response to endogenous DNA damage in human cells."
785 *Proc Natl Acad Sci U S A* 115 (10): 2532-2537. https://doi.org/10.1073/pnas.1715345115.
786 https://www.ncbi.nlm.nih.gov/pubmed/29463760.

787 Holmgren, L., M. S. O'Reilly, and J. Folkman. 1995. "Dormancy of micrometastases: balanced
788 proliferation and apoptosis in the presence of angiogenesis suppression." *Nat Med* 1 (2): 149-
789 53. https://doi.org/10.1038/nm0295-149. https://www.ncbi.nlm.nih.gov/pubmed/7585012.

790 Huang, S. 2021. "Reconciling Non-Genetic Plasticity with Somatic Evolution in Cancer." *Trends*
791 *Cancer* 7 (4): 309-322. https://doi.org/10.1016/j.trecan.2020.12.007.
792 https://www.ncbi.nlm.nih.gov/pubmed/33536158.

793 Ikeda, H., L. J. Old, and R. D. Schreiber. 2002. "The roles of IFN gamma in protection against tumor
794 development and cancer immunoediting." *Cytokine Growth Factor Rev* 13 (2): 95-109.
795 https://doi.org/10.1016/s1359-6101(01)00038-7.
796 https://www.ncbi.nlm.nih.gov/pubmed/11900986.

797 Itahana, K., G. P. Dimri, E. Hara, Y. Itahana, Y. Zou, P. Y. Desprez, and J. Campisi. 2002. "A role
798 for p53 in maintaining and establishing the quiescence growth arrest in human cells." *J Biol*
799 *Chem* 277 (20): 18206-14. https://doi.org/10.1074/jbc.M201028200.
800 https://www.ncbi.nlm.nih.gov/pubmed/11880381.

801 Jager, M., F. Blokzijl, E. Kuijk, J. Bertl, M. Vougioukalaki, R. Janssen, N. Besselink, S. Boymans, J.
802 de Ligt, J. S. Pedersen, J. Hoeijmakers, J. Pothof, R. van Boxtel, and E. Cuppen. 2019.
803 "Deficiency of nucleotide excision repair is associated with mutational signature observed in
804 cancer." *Genome Res* 29 (7): 1067-1077. https://doi.org/10.1101/gr.246223.118.
805 https://www.ncbi.nlm.nih.gov/pubmed/31221724.

806 Jahanban-Esfahlan, R., K. Seidi, M. H. Manjili, A. Jahanban-Esfahlan, T. Javaheri, and P. Zare.
807 2019. "Tumor Cell Dormancy: Threat or Opportunity in the Fight against Cancer." *Cancers*
808 *(Basel)* 11 (8). https://doi.org/10.3390/cancers11081207.
809 https://www.ncbi.nlm.nih.gov/pubmed/31430951.

Jelaković, B., X. Castells, K. Tomić, M. Ardin, S. Karanović, and J. Zavadil. 2015. "Renal cell carcinomas of chronic kidney disease patients harbor the mutational signature of carcinogenic aristolochic acid." *Int J Cancer* 136 (12): 2967-72. https://doi.org/10.1002/ijc.29338. https://www.ncbi.nlm.nih.gov/pubmed/25403517.

Jiménez-Sánchez, A., O. Cast, and M. L. Miller. 2019. "Comprehensive Benchmarking and Integration of Tumor Microenvironment Cell Estimation Methods." *Cancer Res* 79 (24): 6238-6246. https://doi.org/10.1158/0008-5472.CAN-18-3560. https://www.ncbi.nlm.nih.gov/pubmed/31641033.

Katoh, M. 2012. "Function and cancer genomics of FAT family genes (review)." *Int J Oncol* 41 (6): 1913-8. https://doi.org/10.3892/ijo.2012.1669. https://www.ncbi.nlm.nih.gov/pubmed/23076869.

Kim, M. J., C. Cervantes, Y. S. Jung, X. Zhang, J. Zhang, S. H. Lee, S. Jun, L. Litovchick, W. Wang, J. Chen, B. Fang, and J. I. Park. 2021. "PAF remodels the DREAM complex to bypass cell quiescence and promote lung tumorigenesis." *Mol Cell*. https://doi.org/10.1016/j.molcel.2021.02.001. https://www.ncbi.nlm.nih.gov/pubmed/33626321.

Koebel, C. M., W. Vermi, J. B. Swann, N. Zerafa, S. J. Rodig, L. J. Old, M. J. Smyth, and R. D. Schreiber. 2007. "Adaptive immunity maintains occult cancer in an equilibrium state." *Nature* 450 (7171): 903-7. https://doi.org/10.1038/nature06309. https://www.ncbi.nlm.nih.gov/pubmed/18026089.

Krock, B. L., N. Skuli, and M. C. Simon. 2011. "Hypoxia-induced angiogenesis: good and evil." *Genes Cancer* 2 (12): 1117-33. https://doi.org/10.1177/1947601911423654. https://www.ncbi.nlm.nih.gov/pubmed/22866203.

Kundu, A., H. Nam, S. Shelar, D. S. Chandrashekar, G. Brinkley, S. Karki, T. Mitchell, C. B. Livi, P. Buckhaults, R. Kirkman, Y. Tang, G. C. Rowe, S. Wei, S. Varambally, and S. Sudarshan. 2020. "PRDM16 suppresses HIF-targeted gene expression in kidney cancer." *J Exp Med* 217 (6). https://doi.org/10.1084/jem.20191005. https://www.ncbi.nlm.nih.gov/pubmed/32251515.

Leek, J. T., W. E. Johnson, H. S. Parker, A. E. Jaffe, and J. D. Storey. 2012. "The sva package for removing batch effects and other unwanted variation in high-throughput experiments." *Bioinformatics* 28 (6): 882-3. https://doi.org/10.1093/bioinformatics/bts034. https://www.ncbi.nlm.nih.gov/pubmed/22257669.

Leonard, B., G. J. Starrett, M. J. Maurer, A. L. Oberg, M. Van Bockstal, J. Van Dorpe, O. De Wever, J. Helleman, A. M. Sieuwerts, E. M. Berns, J. W. Martens, B. D. Anderson, W. L. Brown, K. R. Kalli, S. H. Kaufmann, and R. S. Harris. 2016. "APOBEC3G Expression Correlates with T-Cell Infiltration and Improved Clinical Outcomes in High-grade Serous Ovarian Carcinoma." *Clin Cancer Res* 22 (18): 4746-55. https://doi.org/10.1158/1078-0432.CCR-15-2910. https://www.ncbi.nlm.nih.gov/pubmed/27016308.

Liu, D., J. Aguirre Ghiso, Y. Estrada, and L. Ossowski. 2002. "EGFR is a transducer of the urokinase receptor initiated signal that is required for in vivo growth of a human carcinoma." *Cancer Cell* 1 (5): 445-57. https://doi.org/10.1016/s1535-6108(02)00072-7. https://www.ncbi.nlm.nih.gov/pubmed/12124174.

Lyu, T., N. Jia, J. Wang, X. Yan, Y. Yu, Z. Lu, R. C. Bast, K. Hua, and W. Feng. 2013. "Expression and epigenetic regulation of angiogenesis-related factors during dormancy and recurrent

853 growth of ovarian carcinoma." *Epigenetics* 8 (12): 1330-46.
854 https://doi.org/10.4161/epi.26675. https://www.ncbi.nlm.nih.gov/pubmed/24135786.

855 MacDonald, J., Y. Ramos-Valdes, P. Perampalam, L. Litovchick, G. E. DiMattia, and F. A. Dick.
856 2017. "A Systematic Analysis of Negative Growth Control Implicates the DREAM Complex
857 in Cancer Cell Dormancy." *Mol Cancer Res* 15 (4): 371-381. https://doi.org/10.1158/1541-
858 7786.MCR-16-0323-T. https://www.ncbi.nlm.nih.gov/pubmed/28031411.

859 Martincorena, I., K. M. Raine, M. Gerstung, K. J. Dawson, K. Haase, P. Van Loo, H. Davies, M. R.
860 Stratton, and P. J. Campbell. 2017. "Universal Patterns of Selection in Cancer and Somatic
861 Tissues." *Cell* 171 (5): 1029-1041.e21. https://doi.org/10.1016/j.cell.2017.09.042.
862 https://www.ncbi.nlm.nih.gov/pubmed/29056346.

863 McGranahan, N., and C. Swanton. 2017. "Clonal Heterogeneity and Tumor Evolution: Past, Present,
864 and the Future." *Cell* 168 (4): 613-628. https://doi.org/10.1016/j.cell.2017.01.018.
865 https://www.ncbi.nlm.nih.gov/pubmed/28187284.

866 Miller, I., M. Min, C. Yang, C. Tian, S. Gookin, D. Carter, and S. L. Spencer. 2018. "Ki67 is a
867 Graded Rather than a Binary Marker of Proliferation versus Quiescence." *Cell Rep* 24 (5):
868 1105-1112.e5. https://doi.org/10.1016/j.celrep.2018.06.110.
869 https://www.ncbi.nlm.nih.gov/pubmed/30067968.

870 Mittal, D., M. M. Gubin, R. D. Schreiber, and M. J. Smyth. 2014. "New insights into cancer
871 immunoediting and its three component phases--elimination, equilibrium and escape." *Curr*
872 *Opin Immunol* 27: 16-25. https://doi.org/10.1016/j.coi.2014.01.004.
873 https://www.ncbi.nlm.nih.gov/pubmed/24531241.

874 Moon, K. R., D. van Dijk, Z. Wang, S. Gigante, D. B. Burkhardt, W. S. Chen, K. Yim, A. V. D.
875 Elzen, M. J. Hirn, R. R. Coifman, N. B. Ivanova, G. Wolf, and S. Krishnaswamy. 2019.
876 "Visualizing structure and transitions in high-dimensional biological data." *Nat Biotechnol* 37
877 (12): 1482-1492. https://doi.org/10.1038/s41587-019-0336-3.
878 https://www.ncbi.nlm.nih.gov/pubmed/31796933.

879 Moserle, L., A. Amadori, and S. Indraccolo. 2009. "The angiogenic switch: implications in the
880 regulation of tumor dormancy." *Curr Mol Med* 9 (8): 935-41.
881 https://doi.org/10.2174/156652409789712800.
882 https://www.ncbi.nlm.nih.gov/pubmed/19925406.

883 Naumov, G. N., E. Bender, D. Zurakowski, S. Y. Kang, D. Sampson, E. Flynn, R. S. Watnick, O.
884 Straume, L. A. Akslen, J. Folkman, and N. Almog. 2006. "A model of human tumor
885 dormancy: an angiogenic switch from the nonangiogenic phenotype." *J Natl Cancer Inst* 98
886 (5): 316-25. https://doi.org/10.1093/jnci/djj068.
887 https://www.ncbi.nlm.nih.gov/pubmed/16507828.

888 Oh, C. W., J. Hoover-Plow, and E. F. Plow. 2003. "The role of plasminogen in angiogenesis in vivo."
889 *J Thromb Haemost* 1 (8): 1683-7. https://doi.org/10.1046/j.1538-7836.2003.00182.x.
890 https://www.ncbi.nlm.nih.gov/pubmed/12911578.

891 Park, S. Y., and J. S. Nam. 2020. "The force awakens: metastatic dormant cancer cells." *Exp Mol*
892 *Med* 52 (4): 569-581. https://doi.org/10.1038/s12276-020-0423-z.
893 https://www.ncbi.nlm.nih.gov/pubmed/32300189.

894 Petrova, V., M. Annicchiarico-Petruzzelli, G. Melino, and I. Amelio. 2018. "The hypoxic tumour
895 microenvironment." *Oncogenesis* 7 (1): 10. https://doi.org/10.1038/s41389-017-0011-9.
896 https://www.ncbi.nlm.nih.gov/pubmed/29362402.

897 Phan, T. G., and P. I. Croucher. 2020. "The dormant cancer cell life cycle." *Nat Rev Cancer* 20 (7):
898 398-411. https://doi.org/10.1038/s41568-020-0263-0.
899 https://www.ncbi.nlm.nih.gov/pubmed/32488200.

900 Polyak, K., Y. Xia, J. L. Zweier, K. W. Kinzler, and B. Vogelstein. 1997. "A model for p53-induced
901 apoptosis." *Nature* 389 (6648): 300-5. https://doi.org/10.1038/38525.
902 https://www.ncbi.nlm.nih.gov/pubmed/9305847.

903 Pugh, C. W., and P. J. Ratcliffe. 2003. "Regulation of angiogenesis by hypoxia: role of the HIF
904 system." *Nat Med* 9 (6): 677-84. https://doi.org/10.1038/nm0603-677.
905 https://www.ncbi.nlm.nih.gov/pubmed/12778166.

906 Qin, L., Y. Xu, G. Ma, L. Liao, Y. Wu, Y. Li, X. Wang, J. Jiang, J. Wang, and J. Xu. 2015. "NCOA1
907 promotes angiogenesis in breast tumors by simultaneously enhancing both HIF1α- and AP-1-
908 mediated VEGFa transcription." *Oncotarget* 6 (27): 23890-904.
909 https://doi.org/10.18632/oncotarget.4341. https://www.ncbi.nlm.nih.gov/pubmed/26287601.

910 Qiu, G. Z., M. Z. Jin, J. X. Dai, W. Sun, J. H. Feng, and W. L. Jin. 2017. "Reprogramming of the
911 Tumor in the Hypoxic Niche: The Emerging Concept and Associated Therapeutic Strategies."
912 *Trends Pharmacol Sci* 38 (8): 669-686. https://doi.org/10.1016/j.tips.2017.05.002.
913 https://www.ncbi.nlm.nih.gov/pubmed/28602395.

914 Ranganathan, A. C., L. Zhang, A. P. Adam, and J. A. Aguirre-Ghiso. 2006. "Functional coupling of
915 p38-induced up-regulation of BiP and activation of RNA-dependent protein kinase-like
916 endoplasmic reticulum kinase to drug resistance of dormant carcinoma cells." *Cancer Res* 66
917 (3): 1702-11. https://doi.org/10.1158/0008-5472.CAN-05-3092.
918 https://www.ncbi.nlm.nih.gov/pubmed/16452230.

919 Rebhandl, S., M. Huemer, F. J. Gassner, N. Zaborsky, D. Hebenstreit, K. Catakovic, E. M.
920 Grössinger, R. Greil, and R. Geisberger. 2014. "APOBEC3 signature mutations in chronic
921 lymphocytic leukemia." *Leukemia* 28 (9): 1929-32. https://doi.org/10.1038/leu.2014.160.
922 https://www.ncbi.nlm.nih.gov/pubmed/24840555.

923 Robbiani, D. F., and M. C. Nussenzweig. 2013. "Chromosome translocation, B cell lymphoma, and
924 activation-induced cytidine deaminase." *Annu Rev Pathol* 8: 79-103.
925 https://doi.org/10.1146/annurev-pathol-020712-164004.
926 https://www.ncbi.nlm.nih.gov/pubmed/22974238.

927 Roberts, S. A., M. S. Lawrence, L. J. Klimczak, S. A. Grimm, D. Fargo, P. Stojanov, A. Kiezun, G.
928 V. Kryukov, S. L. Carter, G. Saksena, S. Harris, R. R. Shah, M. A. Resnick, G. Getz, and D.
929 A. Gordenin. 2013. "An APOBEC cytidine deaminase mutagenesis pattern is widespread in
930 human cancers." *Nat Genet* 45 (9): 970-6. https://doi.org/10.1038/ng.2702.
931 https://www.ncbi.nlm.nih.gov/pubmed/23852170.

932 Rosenthal, R., N. McGranahan, J. Herrero, B. S. Taylor, and C. Swanton. 2016. "DeconstructSigs:
933 delineating mutational processes in single tumors distinguishes DNA repair deficiencies and
934 patterns of carcinoma evolution." *Genome Biol* 17: 31. https://doi.org/10.1186/s13059-016-
935 0893-4. https://www.ncbi.nlm.nih.gov/pubmed/26899170.

936 Sadasivam, S., and J. A. DeCaprio. 2013. "The DREAM complex: master coordinator of cell cycle-
937 dependent gene expression." *Nat Rev Cancer* 13 (8): 585-95. https://doi.org/10.1038/nrc3556.
938 https://www.ncbi.nlm.nih.gov/pubmed/23842645.

939 Semenza, G. L. 2003. "Targeting HIF-1 for cancer therapy." *Nat Rev Cancer* 3 (10): 721-32.
940 https://doi.org/10.1038/nrc1187. https://www.ncbi.nlm.nih.gov/pubmed/13130303.

941 Senft, D., and Z. A. Ronai. 2016. "Immunogenic, cellular, and angiogenic drivers of tumor
942 dormancy--a melanoma view." *Pigment Cell Melanoma Res* 29 (1): 27-42.
943 https://doi.org/10.1111/pcmr.12432. https://www.ncbi.nlm.nih.gov/pubmed/26514653.

944 Shen, S., and J. Clairambault. 2020. "Cell plasticity in cancer cell populations." *F1000Res* 9.
945 https://doi.org/10.12688/f1000research.24803.1.
946 https://www.ncbi.nlm.nih.gov/pubmed/32595946.

947 Shivji, M. K., V. N. Podust, U. Hübscher, and R. D. Wood. 1995. "Nucleotide excision repair DNA
948 synthesis by DNA polymerase epsilon in the presence of PCNA, RFC, and RPA."
949 *Biochemistry* 34 (15): 5011-7. https://doi.org/10.1021/bi00015a012.
950 https://www.ncbi.nlm.nih.gov/pubmed/7711023.

951 Sigismund, S., D. Avanzato, and L. Lanzetti. 2018. "Emerging functions of the EGFR in cancer."
952 *Mol Oncol* 12 (1): 3-20. https://doi.org/10.1002/1878-0261.12155.
953 https://www.ncbi.nlm.nih.gov/pubmed/29124875.

954 Simó-Riudalbas, L., M. Pérez-Salvia, F. Setien, A. Villanueva, C. Moutinho, A. Martínez-Cardús, S.
955 Moran, M. Berdasco, A. Gomez, E. Vidal, M. Soler, H. Heyn, A. Vaquero, C. de la Torre, S.
956 Barceló-Batllori, A. Vidal, L. Roz, U. Pastorino, K. Szakszon, G. Borck, C. S. Moura, F.
957 Carneiro, I. Zondervan, S. Savola, R. Iwakawa, T. Kohno, J. Yokota, and M. Esteller. 2015.
958 "KAT6B Is a Tumor Suppressor Histone H3 Lysine 23 Acetyltransferase Undergoing
959 Genomic Loss in Small Cell Lung Cancer." *Cancer Res* 75 (18): 3936-45.
960 https://doi.org/10.1158/0008-5472.CAN-14-3702.
961 https://www.ncbi.nlm.nih.gov/pubmed/26208904.

962 Stenglein, M. D., M. B. Burns, M. Li, J. Lengyel, and R. S. Harris. 2010. "APOBEC3 proteins
963 mediate the clearance of foreign DNA from human cells." *Nat Struct Mol Biol* 17 (2): 222-9.
964 https://doi.org/10.1038/nsmb.1744. https://www.ncbi.nlm.nih.gov/pubmed/20062055.

965 Swanton, C., N. McGranahan, G. J. Starrett, and R. S. Harris. 2015. "APOBEC Enzymes: Mutagenic
966 Fuel for Cancer Evolution and Heterogeneity." *Cancer Discov* 5 (7): 704-12.
967 https://doi.org/10.1158/2159-8290.CD-15-0344.
968 https://www.ncbi.nlm.nih.gov/pubmed/26091828.

969 Tate, J. G., S. Bamford, H. C. Jubb, Z. Sondka, D. M. Beare, N. Bindal, H. Boutselakis, C. G. Cole,
970 C. Creatore, E. Dawson, P. Fish, B. Harsha, C. Hathaway, S. C. Jupe, C. Y. Kok, K. Noble, L.
971 Ponting, C. C. Ramshaw, C. E. Rye, H. E. Speedy, R. Stefancsik, S. L. Thompson, S. Wang,
972 S. Ward, P. J. Campbell, and S. A. Forbes. 2019. "COSMIC: the Catalogue Of Somatic
973 Mutations In Cancer." *Nucleic Acids Res* 47 (D1): D941-D947.
974 https://doi.org/10.1093/nar/gky1015. https://www.ncbi.nlm.nih.gov/pubmed/30371878.

975 Temko, D., I. P. M. Tomlinson, S. Severini, B. Schuster-Böckler, and T. A. Graham. 2018. "The
976 effects of mutational processes and selection on driver mutations across cancer types." *Nat*
977 *Commun* 9 (1): 1857. https://doi.org/10.1038/s41467-018-04208-6.
978 https://www.ncbi.nlm.nih.gov/pubmed/29748584.

979 Teng, M. W., J. B. Swann, C. M. Koebel, R. D. Schreiber, and M. J. Smyth. 2008. "Immune-
980 mediated dormancy: an equilibrium with cancer." *J Leukoc Biol* 84 (4): 988-93.
981 https://doi.org/10.1189/jlb.1107774. https://www.ncbi.nlm.nih.gov/pubmed/18515327.

982 Theodoropoulos, V. E., A. C.h Lazaris, F. Sofras, I. Gerzelis, V. Tsoukala, I. Ghikonti, K. Manikas,
983 and I. Kastriotis. 2004. "Hypoxia-inducible factor 1 alpha expression correlates with
984 angiogenesis and unfavorable prognosis in bladder cancer." *Eur Urol* 46 (2): 200-8.

985 https://doi.org/10.1016/j.eururo.2004.04.008.
986 https://www.ncbi.nlm.nih.gov/pubmed/15245814.

987 Tommasini-Ghelfi, S., K. Murnan, F. M. Kouri, A. S. Mahajan, J. L. May, and A. H. Stegh. 2019.
988 "Cancer-associated mutation and beyond: The emerging biology of isocitrate dehydrogenases
989 in human disease." *Sci Adv* 5 (5): eaaw4543. https://doi.org/10.1126/sciadv.aaw4543.
990 https://www.ncbi.nlm.nih.gov/pubmed/31131326.

991 Tummers, B., and D. R. Green. 2017. "Caspase-8: regulating life and death." *Immunol Rev* 277 (1):
992 76-89. https://doi.org/10.1111/imr.12541. https://www.ncbi.nlm.nih.gov/pubmed/28462525.

993 Turcan, S., D. Rohle, A. Goenka, L. A. Walsh, F. Fang, E. Yilmaz, C. Campos, A. W. Fabius, C. Lu,
994 P. S. Ward, C. B. Thompson, A. Kaufman, O. Guryanova, R. Levine, A. Heguy, A. Viale, L.
995 G. Morris, J. T. Huse, I. K. Mellinghoff, and T. A. Chan. 2012. "IDH1 mutation is sufficient
996 to establish the glioma hypermethylator phenotype." *Nature* 483 (7390): 479-83.
997 https://doi.org/10.1038/nature10866. https://www.ncbi.nlm.nih.gov/pubmed/22343889.

998 Vogelstein, B., D. Lane, and A. J. Levine. 2000. "Surfing the p53 network." *Nature* 408 (6810): 307-
999 10. https://doi.org/10.1038/35042675. https://www.ncbi.nlm.nih.gov/pubmed/11099028.

1000 Wall, L., F. Burke, J. F. Smyth, and F. Balkwill. 2003. "The anti-proliferative activity of interferon-
1001 gamma on ovarian cancer: in vitro and in vivo." *Gynecol Oncol* 88 (1 Pt 2): S149-51.
1002 https://doi.org/10.1006/gyno.2002.6707. https://www.ncbi.nlm.nih.gov/pubmed/12586108.

1003 Wang, F. X., J. Huang, H. Zhang, and X. Ma. 2008. "APOBEC3G upregulation by alpha interferon
1004 restricts human immunodeficiency virus type 1 infection in human peripheral plasmacytoid
1005 dendritic cells." *J Gen Virol* 89 (Pt 3): 722-730. https://doi.org/10.1099/vir.0.83530-0.
1006 https://www.ncbi.nlm.nih.gov/pubmed/18272764.

1007 Wang, H. F., S. S. Wang, M. C. Huang, X. H. Liang, Y. J. Tang, and Y. L. Tang. 2019. "Targeting
1008 Immune-Mediated Dormancy: A Promising Treatment of Cancer." *Front Oncol* 9: 498.
1009 https://doi.org/10.3389/fonc.2019.00498. https://www.ncbi.nlm.nih.gov/pubmed/31297335.

1010 Wang, S., M. Jia, Z. He, and X. S. Liu. 2018. "APOBEC3B and APOBEC mutational signature as
1011 potential predictive markers for immunotherapy response in non-small cell lung cancer."
1012 *Oncogene* 37 (29): 3924-3936. https://doi.org/10.1038/s41388-018-0245-9.
1013 https://www.ncbi.nlm.nih.gov/pubmed/29695832.

1014 Wang, Shixiang, Huimin Li, Minfang Song, Zaoke He, Tao Wu, Xuan Wang, Ziyu Tao, Kai Wu, and
1015 Xue-Song Liu. 2020. "Copy number signature analyses in prostate cancer reveal distinct
1016 etiologies and clinical outcomes." *medRxiv*: 2020.04.27.20082404.
1017 https://doi.org/10.1101/2020.04.27.20082404.
1018 http://medrxiv.org/content/early/2020/04/29/2020.04.27.20082404.abstract.

1019 Watnick, R. S., R. K. Rodriguez, S. Wang, A. L. Blois, A. Rangarajan, T. Ince, and R. A. Weinberg.
1020 2015. "Thrombospondin-1 repression is mediated via distinct mechanisms in fibroblasts and
1021 epithelial cells." *Oncogene* 34 (22): 2823-35. https://doi.org/10.1038/onc.2014.228.
1022 https://www.ncbi.nlm.nih.gov/pubmed/25109329.

1023 Wherry, E. J., and M. Kurachi. 2015. "Molecular and cellular insights into T cell exhaustion." *Nat*
1024 *Rev Immunol* 15 (8): 486-99. https://doi.org/10.1038/nri3862.
1025 https://www.ncbi.nlm.nih.gov/pubmed/26205583.

1026 White, D. E., N. A. Kurpios, D. Zuo, J. A. Hassell, S. Blaess, U. Mueller, and W. J. Muller. 2004.
1027 "Targeted disruption of beta1-integrin in a transgenic mouse model of human breast cancer

1028 reveals an essential role in mammary tumor induction." *Cancer Cell* 6 (2): 159-70.
1029 https://doi.org/10.1016/j.ccr.2004.06.025. https://www.ncbi.nlm.nih.gov/pubmed/15324699.

1030 Winter, S. C., F. M. Buffa, P. Silva, C. Miller, H. R. Valentine, H. Turley, K. A. Shah, G. J. Cox, R.
1031 J. Corbridge, J. J. Homer, B. Musgrove, N. Slevin, P. Sloan, P. Price, C. M. West, and A. L.
1032 Harris. 2007. "Relation of a hypoxia metagene derived from head and neck cancer to
1033 prognosis of multiple cancers." *Cancer Res* 67 (7): 3441-9. https://doi.org/10.1158/0008-
1034 5472.CAN-06-3322. https://www.ncbi.nlm.nih.gov/pubmed/17409455.

1035 Yamazaki, H., K. Shirakawa, T. Matsumoto, S. Hirabayashi, Y. Murakawa, M. Kobayashi, A. D.
1036 Sarca, Y. Kazuma, H. Matsui, W. Maruyama, H. Fukuda, R. Shirakawa, K. Shindo, M. Ri, S.
1037 Iida, and A. Takaori-Kondo. 2019. "Endogenous APOBEC3B Overexpression Constitutively
1038 Generates DNA Substitutions and Deletions in Myeloma Cells." *Sci Rep* 9 (1): 7122.
1039 https://doi.org/10.1038/s41598-019-43575-y.
1040 https://www.ncbi.nlm.nih.gov/pubmed/31073151.

1041 Ye, D., S. Ma, Y. Xiong, and K. L. Guan. 2013. "R-2-hydroxyglutarate as the key effector of IDH
1042 mutations promoting oncogenesis." *Cancer Cell* 23 (3): 274-6.
1043 https://doi.org/10.1016/j.ccr.2013.03.005. https://www.ncbi.nlm.nih.gov/pubmed/23518346.

1044 Yi, J. S., M. A. Cox, and A. J. Zajac. 2010. "T-cell exhaustion: characteristics, causes and
1045 conversion." *Immunology* 129 (4): 474-81. https://doi.org/10.1111/j.1365-2567.2010.03255.x.
1046 https://www.ncbi.nlm.nih.gov/pubmed/20201977.

1047 Yuan, S., R. J. Norgard, and B. Z. Stanger. 2019. "Cellular Plasticity in Cancer." *Cancer Discov* 9
1048 (7): 837-851. https://doi.org/10.1158/2159-8290.CD-19-0015.
1049 https://www.ncbi.nlm.nih.gov/pubmed/30992279.

1050 Zhang, T., T. Otevrel, Z. Gao, S. M. Ehrlich, J. Z. Fields, and B. M. Boman. 2001. "Evidence that
1051 APC regulates survivin expression: a possible mechanism contributing to the stem cell origin
1052 of colon cancer." *Cancer Res* 61 (24): 8664-7.
1053 https://www.ncbi.nlm.nih.gov/pubmed/11751382.

1054 Zhao, X., J. Liu, S. Ge, C. Chen, S. Li, X. Wu, X. Feng, Y. Wang, and D. Cai. 2019. "Saikosaponin
1055 A Inhibits Breast Cancer by Regulating Th1/Th2 Balance." *Front Pharmacol* 10: 624.
1056 https://doi.org/10.3389/fphar.2019.00624. https://www.ncbi.nlm.nih.gov/pubmed/31214035.

1057 Zhi, X., J. Tao, K. Xie, Y. Zhu, Z. Li, J. Tang, W. Wang, H. Xu, J. Zhang, and Z. Xu. 2014. "MUC4-
1058 induced nuclear translocation of β-catenin: a novel mechanism for growth, metastasis and
1059 angiogenesis in pancreatic cancer." *Cancer Lett* 346 (1): 104-13.
1060 https://doi.org/10.1016/j.canlet.2013.12.021.
1061 https://www.ncbi.nlm.nih.gov/pubmed/24374017.

1062

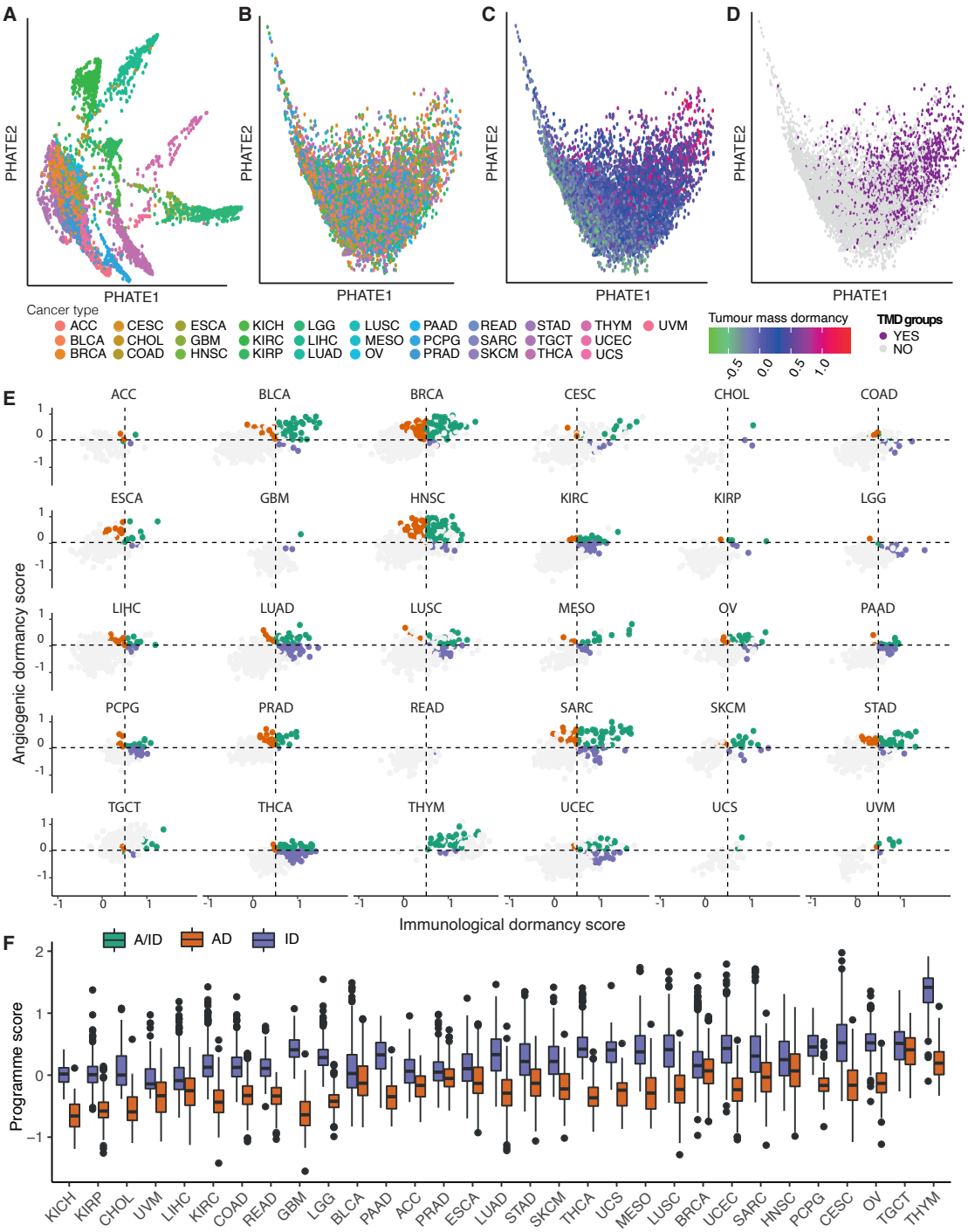

Figure 1. The pan-cancer landscape of TMD. (A-D) PHATE dimensionality reduction applied to 9,631 primary tumor samples based on the expression of genes within the TMD and exhaustion programmes before **(A)** and after **(B-D)** removal of tissue specific expression patterns. The maps are coloured by their corresponding tissue type **(A-B)**, TMD programme score **(C)** and TMD status **(D)**. **(E)** Relationship between immunological and angiogenic programme scores within individual TCGA cancer tissues. Samples are colored by their angiogenic (orange, AD), immunological (purple, ID) and tumour mass (green, A/ID) dormancy status. Samples showing no evidence of TMD are coloured in light grey. Horizontal and vertical dashed lines represent the upper quartile of the pan-cancer angiogenic and immunological dormancy programme scores, respectively. KICH was not plotted because it lacked TMD samples. **(F)** Variation in immunological and angiogenic dormancy scores across primary tumor TCGA samples stratified by tissue type. The tissues are sorted by their TMD levels.

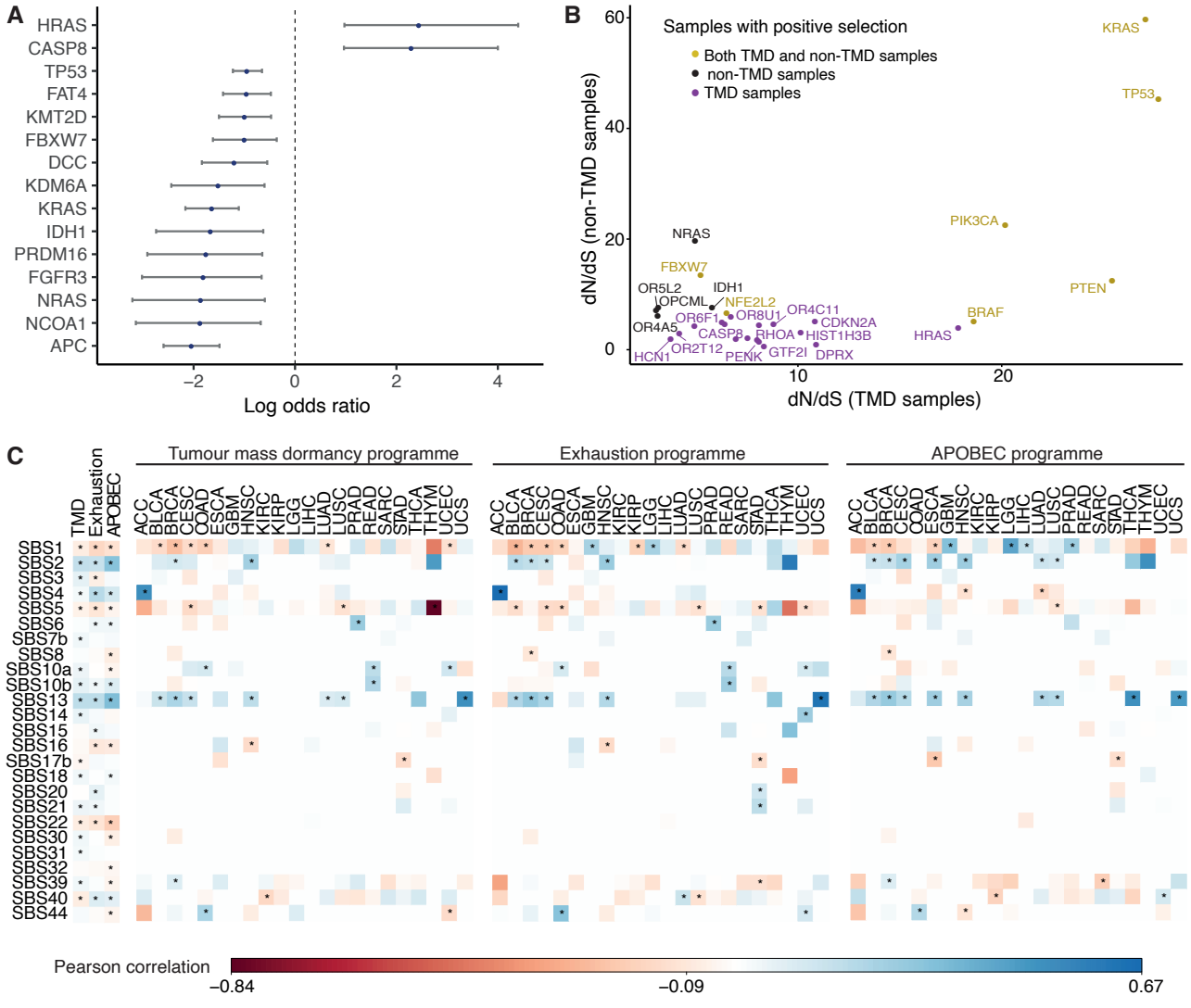

Figure 2. Genomic drivers and mutational processes linked with TMD. (A) Genes presenting an enrichment or depletion of mutations within high TMD samples. Blue circles represent odds ratios on a log2 scale and the confidence intervals for each of the individual Fisher's exact tests are depicted. **(B)** Genes showing signals of positive selection in samples with high (purple) and low (black) TMD, as well as across both groups (yellow). **(C)** Matrices depicting the Person correlation between mutational signatures and the TMD, exhaustion and APOBEC programmes, both pan-cancer (first 3 columns) and within individual cancer tissues. Statistically significant correlations ($p<0.05$) are highlighted with an asterisk. Only signatures with at least one significant correlation are shown.

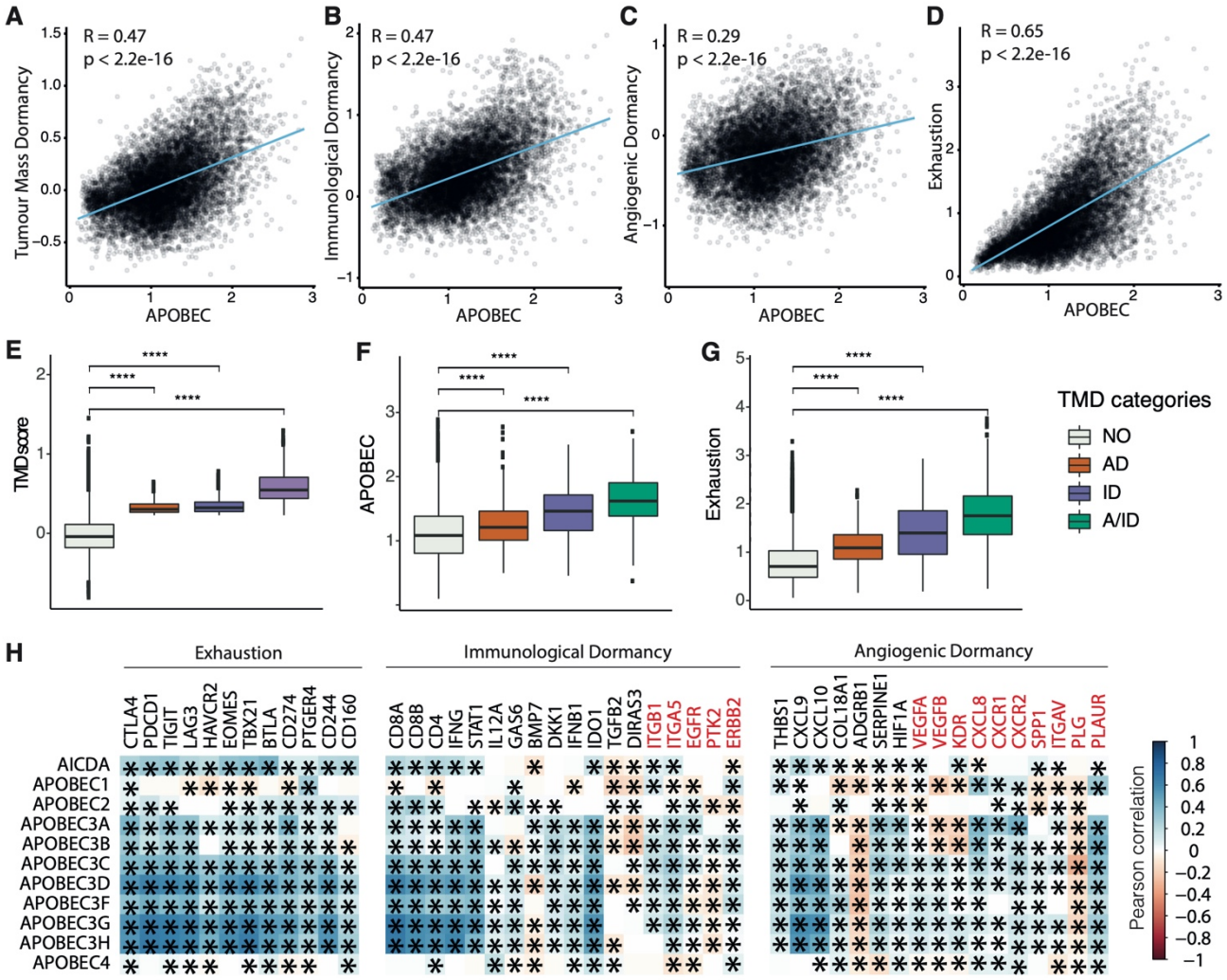

Figure 3. TMD and exhaustion programmes correlate with APOBEC transcriptional activity. (A-D) Pan-cancer correlation between the activity of the APOBEC programme and **(A)** TMD, **(B)** immunological dormancy, **(C)** angiogenic dormancy and **(D)** exhaustion programmes. **(E-G)** TMD, APOBEC and exhaustion programme scores compared between samples with angiogenic dormancy (AD), immunological dormancy (ID), both angiogenic and immunological dormancy (A/ID) and expanding tumours without evidence of TMD (NO); **** p<0.00001. **(H)** Pan-cancer correlation between individual genes in the dormancy and exhaustion programmes and APOBEC/AID enzyme family gene expression. Genes downregulated in the immunological and angiogenic dormancy programmes are shown in red. Significant correlations are marked with an asterisk.

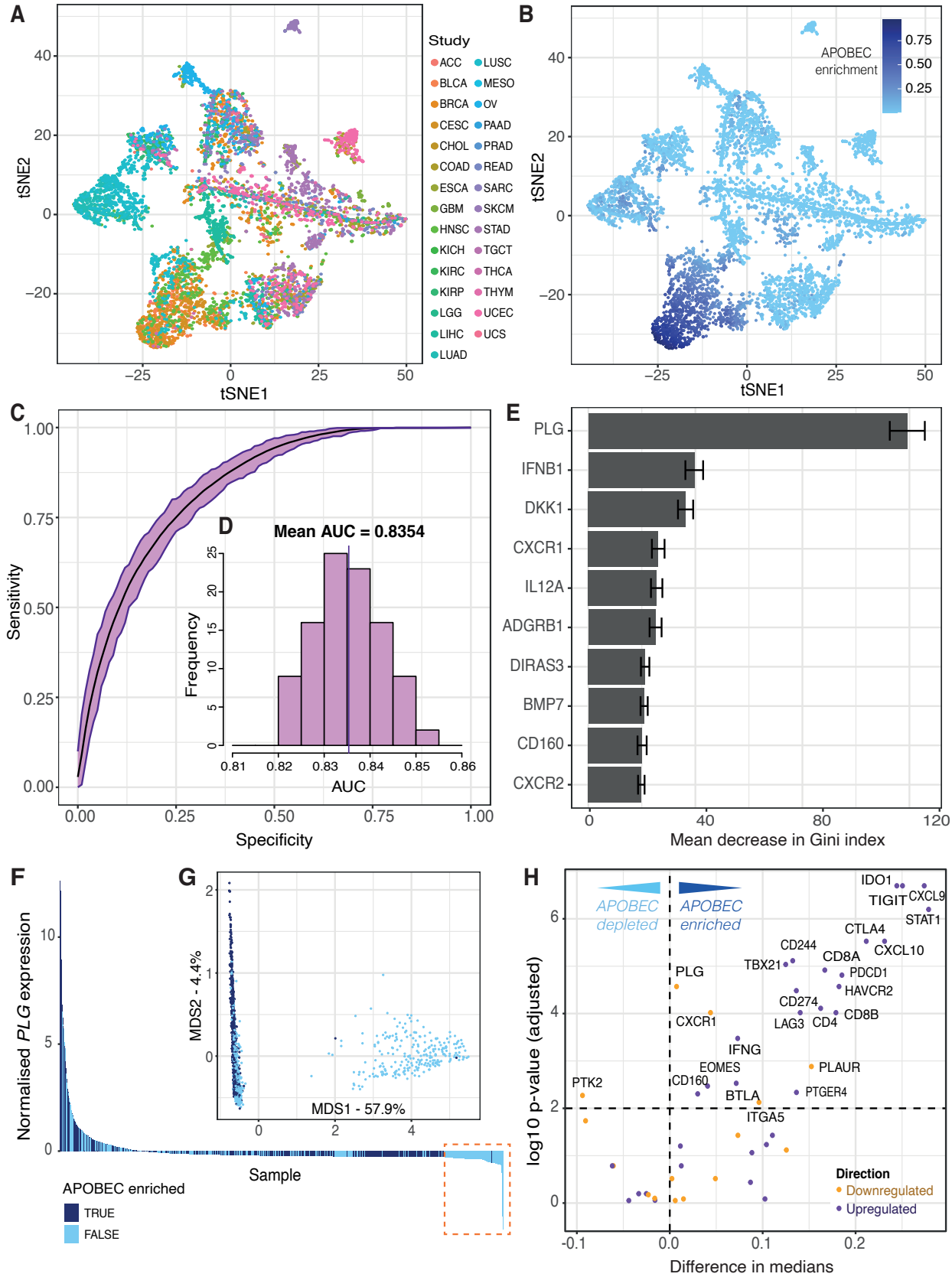

Figure 4. TMD and exhaustion programmes distinguish an APOBEC mutagenesis cluster. tSNE dimensionality reduction of 6,410 primary tumour samples based on single-base substitution signature

1098 profiles labelled by **(A)** TCGA study and **(B)** the total contribution of mutations from APOBEC
1099 signatures SBS2 and SBS13. **(C)** Receiver operating characteristic (ROC) curves of 100 random forest
1100 classifiers of APOBEC signature enrichment based on expression of genes involved in the TMD and
1101 exhaustion programmes. **(D)** Distribution of Area Under Curve (AUC) values across all 100 random
1102 forest classifiers. **(E)** The top 10 ranked genes with highest importance for APOBEC signature
1103 enrichment classification, ranked by mean associated decrease in Gini index across all 100 classifiers.
1104 **(F)** Waterfall plot displaying samples included in an exemplary classifier ranked by normalised *PLG*
1105 expression, coloured by APOBEC enrichment labels. The dashed orange box highlights the subset of
1106 samples with low PLG expression and marked depletion of APOBEC signatures. **(G)** Multidimensional
1107 scaling plot displaying samples included in the exemplary classifier. **(H)** Volcano plot displaying the
1108 difference in median normalised expression for each gene involved in the TMD and exhaustion
1109 programmes between APOBEC-enriched and non-enriched groups, coloured by anticipated direction
1110 of regulation. Differences in medians above 0 correspond to an increase in expression in the APOBEC-
1111 enriched group. Genes with a difference in median <0 would instead be higher expressed in the non-
1112 enriched cluster (APOBEC depleted). A significance cut-off of $p<0.01$ was applied after Benjamini-
1113 Hochberg multiple testing correction.

1114

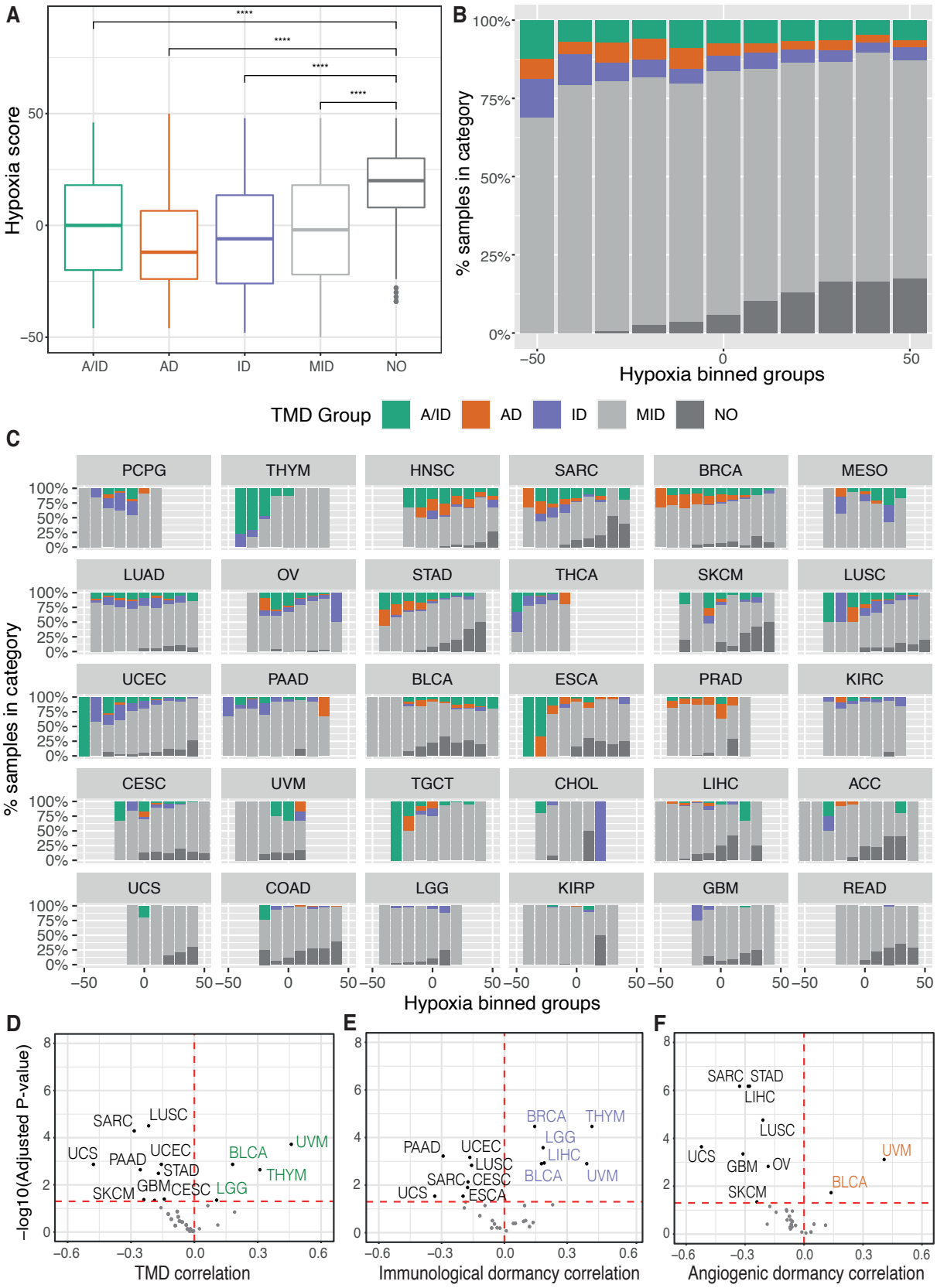

Figure 5. TMD is reduced in the context of hypoxia. (A) Comparison of hypoxia scores across samples falling within distinct TMD categories: both angiogenic and immunological dormancy (A/ID),

1118 angiogenic dormancy (AD), immunological dormancy (ID), slowly expanding tumours (MID),
1119 expanding tumours without evidence of TMD (NO). **(B-C)** Distributions of dormancy status within
1120 hypoxia groups, defined by binning the hypoxia scores into intervals of 10: **(B)** pan-cancer, and **(C)** by
1121 TCGA cancer tissue, arranged in descending proportion of dormant samples. KICH was not plotted
1122 because it lacked TMD samples. **(D-F)** Volcano plots displaying the cancer-study-specific Pearson
1123 correlations of **(D)** TMD, **(E)** immunogenic dormancy and **(F)** angiogenic dormancy programme scores
1124 against hypoxia scores. Cancers showing an increased dormancy in the context of hypoxia are
1125 highlighted in corresponding colours, while cancers with high dormancy in normoxic conditions are
1126 depicted in black.

1127

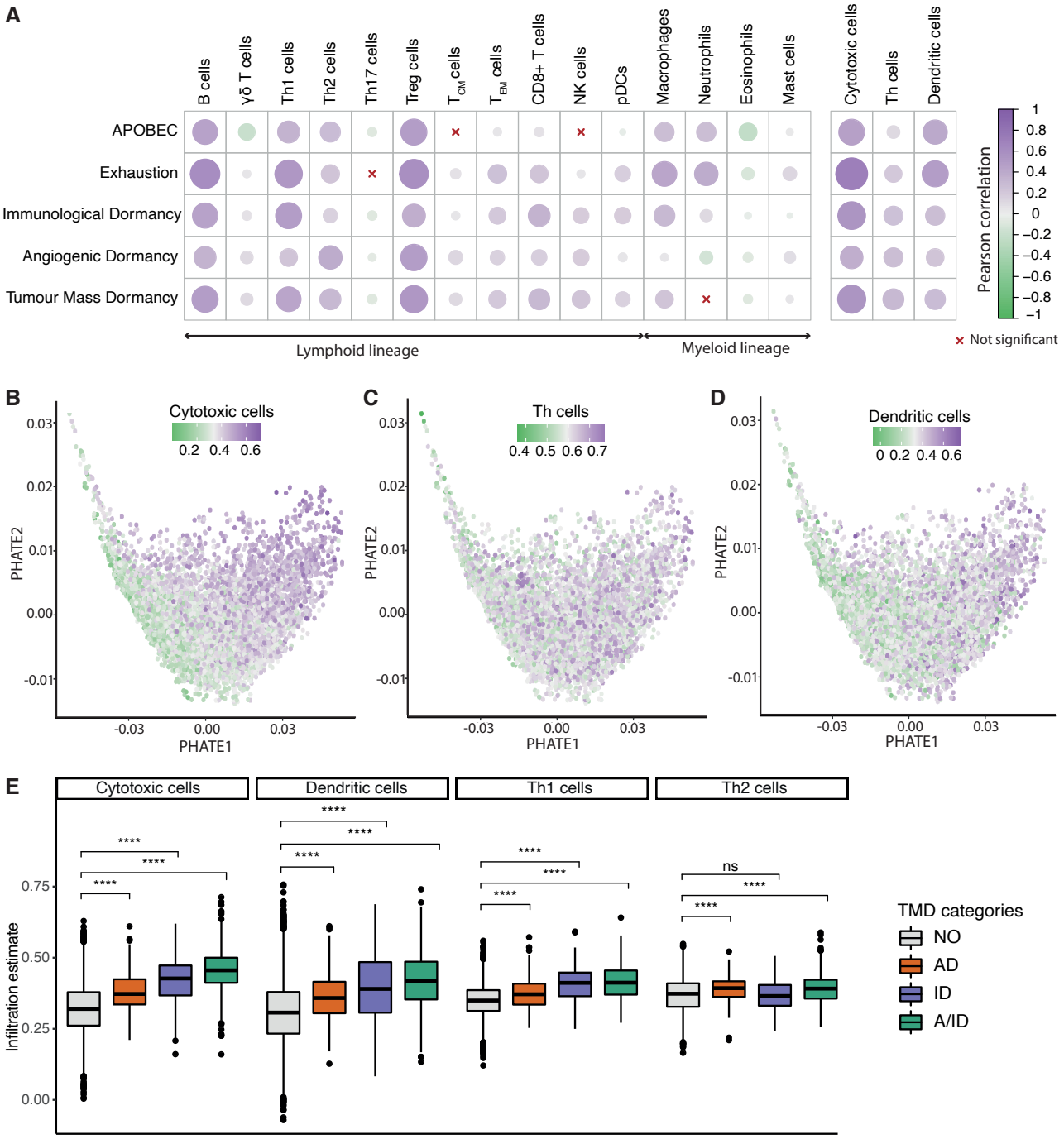

Figure 6. Tumour microenvironment activity correlates with the TMD programme. (A) Correlation between cell infiltration estimates and the APOBEC, exhaustion and dormancy programme scores across the TCGA primary tumor samples. The three broader categories on the right hand side summarise the combined marker expression for all cytotoxic, T helper and dendritic cells. **(B-D)** PHATE dimensionality reduction of 9,631 primary tumor samples, based on the expression of genes driving the TMD and exhaustion programmes, with removal of tissue specific expression patterns and coloured by **(B)** cytotoxic cell enrichment score, **(C)** Th cell enrichment score and **(D)** dendritic cell enrichment score. **(E)** Cytotoxic T cell, Th1/Th2 and dendritic cell abundance compared between samples with angiogenic dormancy (AD), immunological dormancy (ID), both angiogenic and immunological dormancy (A/ID) and samples without TMD (NO); **** $p<0.00001$.

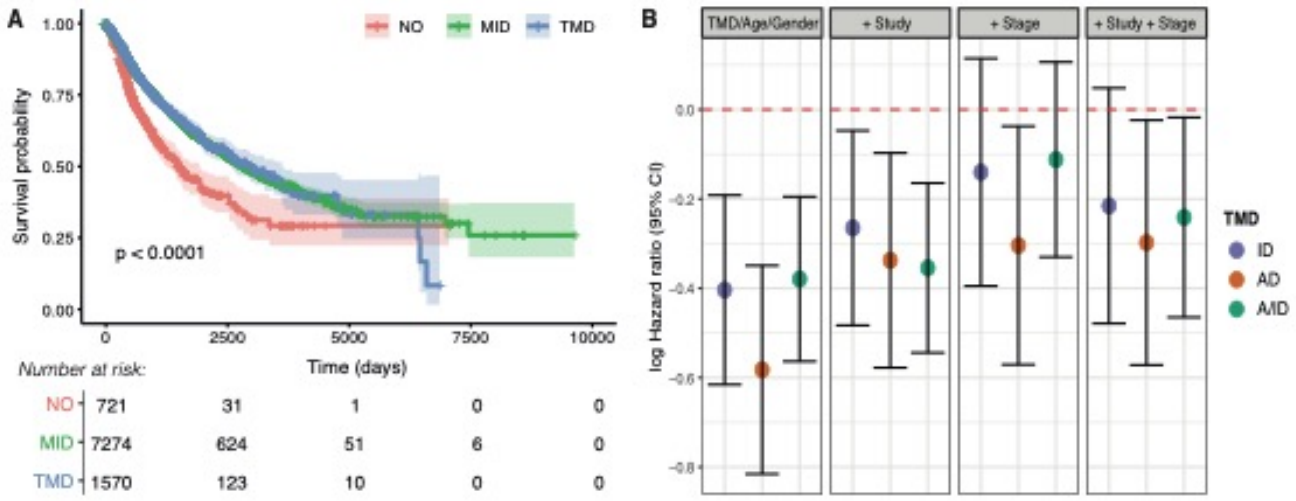

Figure 7. TMD is linked with better prognosis pan-cancer. (A) Overall survival compared between tumours with distinct levels of TMD: strong evidence for TMD (TMD), middle/weak evidence (MID) and no evidence (NO). The number of patients at risk for the corresponding time points are displayed below. **(B)** Log hazard ratios of survival for tumours with angiogenic dormancy (AD), immunological dormancy (ID), both angiogenic and immunological dormancy (A/ID) compared to the 'NO' dormancy category, whilst accounting for age and gender, followed by the inclusion of TCGA study, tumour stage (early/late), and both TCGA study and tumour stage.